Supporting Information

Table of Contents

I. Conditions Screening for a One-pot Synthesis of α-Haloglycine Esters 4a-c.

Table SI-1: One-pot Synthesis of α-Haloglycine Esters **4a-c**

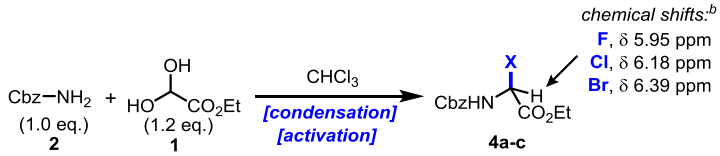

Entry	Promoter (eq.)	Temp	Time	Yield (%)[a]
1	AcCl (3.0) AcOH (0.1)	RT 60 °C	48 h 11 h	**4b** (62) **4b** (100)
2	$SOCl_2$ (3.0)	RT 60 °C	15 h 6 h	**4b** (100) **4b** (100)
3	$SiCl_4$ (1.5)	35 °C	24 h	**4b** (100)
4	BCl_3 (1.0)	0 °C	1 h	**4b** (0)[c]
5	TMSCl (3.0)	RT	60 h	**4b** (89)
6	$(CO)_2Cl_2$ (3.0)	RT	18 h	**4b** (94)
7	AcBr (3.0) AcOH (0.1)	RT	6.5 h	**4c** (100)
8	$SOBr_2$ (3.0)	-20 °C	15 mins	**4c** (100)
9	TMSBr (3.0)	RT	4 h	**4c** (100)
10	BzF (3.0) BzOH (0.1)	0 °C to 60 °C	72 h	**4a** (0)[d]
11	Et_2NSF_3 (3.0)	0 °C to RT	72 h	**4a** (0)
12[e]	Et_2NSF_3 (3.0) AcOH(0.1)	40 °C then -78 °C	15 h then 2 h	**4a** (100)

[a] Yields determined by ^{1}H NMR on crude reaction mixtures using mesitylene as internal standard. [b] ^{1}H NMR recorded in CD_3CN, $^{\alpha}$H: **4a-F**, δ 5.95 ppm (dd, *J* = 9.5, 53.7 Hz); **4b-Cl**, δ 6.18 ppm (d, *J* = 10.4 Hz); **4c-Br**, δ 6.39 ppm (d, *J* = 10.8 Hz). [c] Complete decompostion of starting material Cbz-carbamate **2** was observed in presence of BCl_3. [d] Hemiaminal **3** was formed (25% conversion). [e] Experiment run in CH_2Cl_2 with a stepwise protocol for condensation/deoxyfluorination.

Preliminary kinetic profiling for the reactions presented in the Table above (SI-1) have been obtained by reaction advancement monitoring using 1H NMR via the following 2 protocols:

Protocol A in $CHCl_3$. All reactions were performed in flamed dry scintillation vials (1 drum) equipped with a stirring bar and placed under an inert atmosphere of argon. The vial was initially charged with benzyl carbamate **2** (76 mg, 0.5 mmol, 1.0 eq.) in freshly distilled $CHCl_3$ (5.0 mL) followed ethyl glyoxylate **1** (*c.a.* 50% in toluene, 145 µL, 0.6 mmol, 1.2 eq.) and finally the promoter with the equivalent needed (*e.g.* **Table SI-2**: entries 2-3, $SOCl_2$, 110 µL, 1.5 mmol, 3.0 eq.). The main reaction mixture was then rapidly and accurately transferred and partitioned into 10-15 flamed dry scintillation vials under argon (500 µL of reaction mixture in each vial) with a dry

syringe. Each vial will be used to obtain one kinetic data point to avoid hydrolysis that occurred during transfer. The vial was evaporated at the desired reaction time (see **Table SI-2**) using the rotary evaporator (caution: bath at 0°C) and short period on high vacuum to obtain the different samples and data points of reaction advancement. Note: As soon as the reaction solvent and promoter have been removed under vacuum the reaction does not progress further and the products proved to be stable for several hours as long as the sample was protected from moisture.

Recording data points to assess the reaction course: In a dry flamed vial under argon, the internal standard mesitylene (60 mg) was accurately weighted and dissolved in the NMR solvent CD_3CN (5 mL). This solvent mixture was then added to the sample (400 µL) and the NMR spectrum were recorded in the hour to avoid sample hydrolysis and decomposition (especially frequent in Florida).

Protocol B: *in-situ* protocol in $CDCl_3$. All reactions were performed in flamed dry scintillation vials (1 drum) equipped with a stirring bar and placed under an inert atmosphere of argon. The vial was initially charged with benzyl carbamate **2** (76 mg, 0.5 mmol, 1.0 eq.), mesitylene as the internal standard (60 mg, 0.5 mmol, 1.0 equiv.) in freshly prepared $CDCl_3$ (5 mL passed through a plug of neutral alumina ~1.0 g) followed by ethyl glyoxylate **1** (*c.a.* 50% in toluene, 145 µL, 0.6 mmol, 1.2 eq.) and finally the promoter with the equivalents needed (*e.g.* **Table SI-2** entry 1, TMSCl, 191 µL, 1.5 mmol, 3.0 eq.). The reaction mixture was then rapidly partitioned into 3 or 4 flamed dry scintillation vials under argon (~1.5 mL of reaction mixture in each vial; vial #1 to vial #4) with a dry syringe because of air- and moisture-sensitivity. 4 Aliquots were taken from vial #1 and ^1H NMR were recorded, then the next 4 samples were taken from vial #2 (to avoid hydrolysis artifacts), and so one, and ^1H NMR were recorded until the end of the reaction.

Recording data points to assess the reaction course: At specific times (see **Table SI-2**), an aliquot of the reaction mixture (150 µL) was transferred using a dry syringe to a flame dried NMR tube and CD_3CN (300 µL) was added to the sample (450 µL total volume per tube) then the NMR tube was frozen to -78°C for a couple of minutes to allow transportation to the NMR facility. The temperature of the NMR tube was raised back to RT before the ^1H NMR spectrum was recorded.

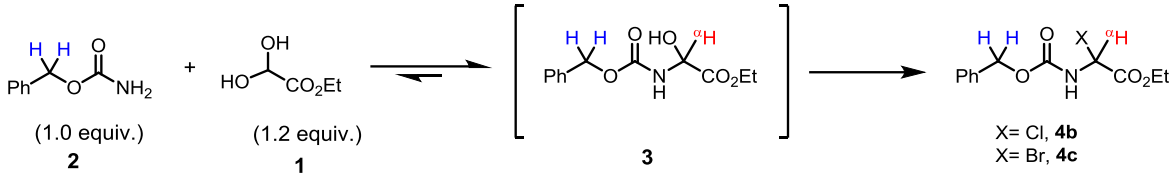

Table SI-2. Kinetic data obtained by ^{1}H NMR for the synthesis of α-haloglycine ester 4b-c

Entry	Solvent, Temp	Promoter	Time (h)	Conversion calculated by signal integrations					% Conversion Avg.	Δ%
				Chloroaminal (**4b**)		Hemiaminal (**3**)		CBz-NH_2 (**2**)		
				$^{\alpha}$H	CH_2	$^{\alpha}$H	CH_2	CH_2		
1[a]	$CDCl_3$, RT	TMSCl	0	-	-	-	-	100	100 (**2**)	9
			0.25	-	-	10	9	91	9(**3**), 91 (**2**)	8
			0.5	-	-	12	11	88	12 (**3**), 88 (**2**)	10
			0.75	-	-	16	11	86	14 (**3**), 86 (**2**)	10
			1	-	-	17	14	85	15 (**3**), 85 (**2**)	11
			1.5	-	-	20	17	81	19 (**3**), 81 (**2**)	9
			2	2	3	24	22	74	2 (**4**), 23 (**3**), 74 (**2**)	13
			2.5	3	5	28	27	68	4 (**4**),28 (**3**), 68 (**2**)	8
			3	3	7	32	30	64	5 (**4**),31 (**3**), 64 (**2**)	14
			5.5	9	12	47	49	42	10 (**4**),48 (**3**), 42 (**2**)	12
			12	25	42	51	60	12	33 (**4**),55 (**3**), 12 (**2**)	13
			26	66	74	28	32	0	70 (**4**),30 (**3**)	11
			36	80	85	17	17	0	83 (**4**),17 (**3**)	7
			48	82	94	9	13	0	88 (**4**),12 (**3**)	11
			60	85	93	5	7	0	89 (**4**),11 (**3**)	14
2[b]	$CHCl_3$, RT	$SOCl_2$	0	-	-	-	-	100	100 (**2**)	0
			1	9	-	54	39	45	9 (**4**), 46 (**3**), 45 (**2**)	6
			2	24	25	61	40	25	25 (**4**), 50 (**3**), 25 (**2**)	7
			4	43	48	48	44	8	46 (**4**), 46 (**3**), 8 (**2**)	8
			5	75	68	28	-	0	72 (**4**), 28 (**3**), 0 (**2**)	7
			6	74	79	23	25	0	77 (**4**), 23 (**3**), 0 (**2**)	4
			7	75	81	24	19	0	78 (**4**), 22 (**3**), 0 (**2**)	3
			15	100	100	0	0	0	100 (**4**), 0 (**3**), 0 (**2**)	2
3[b]	$CHCl_3$, 60 °C	$SOCl_2$	0	-	-	-	-	100	100 (**2**)	0
			1	35	39	40	37	24	37 (**4**), 38 (**3**), 24 (**2**)	6
			2	78	73	23	31	10	76 (**4**), 27 (**3**), 10 (**2**)	2
			3	78	83	14	21	2	80 (**4**), 18 (**3**), 2 (**2**)	7
			4	83	85	15	17	0	84 (**4**), 16 (**3**), 0 (**2**)	3
			6	101	99	0	0	0	100 (**4**), 0 (**3**), 0 (**2**)	3

Table SI-2. ***Continued***

4[a]	$CDCl_3$, 35 °C	$SiCl_4$	0	-	-	0	0	100	100 (**2**)	9
			0.25	-	-	0	0	100	100 (**2**)	4
			0.5	1	9	0	0	95	5 (**4**), 95 (**2**)	11
			0.75	6	14	0	0	85	10 (**4**), 90 (**2**)	11
			1	10	13	0	0	80	13 (**4**),87 (**2**)	6
			1.25	10	14	0	0	68	15 (**4**),85 (**2**)	1
			1.5	18	23	0	0	72	22 (**4**), 78 (**2**)	7
			1.75	19	26	0	0	67	25 (**4**), 75 (**2**)	6
			2	24	28	0	0	64	29 (**4**), 71 (**2**)	4
			2.5	29	32	0	0	59	34 (**4**), 66 (**2**)	4
			3	30	42	0	0	65	36 (**4**), 65 (**2**)	14
			3.5	33	41	0	0	56	40 (**4**), 60 (**2**)	8
			4	33	46	0	0	62	40 (**4**), 60 (**2**)	7
			4.5	39	47	0	0	60	42 (**4**), 58 (**2**)	11
			5	43	48	0	0	55	45 (**4**), 55 (**2**)	13
			5.5	44	53	0	0	54	48 (**4**), 52 (**2**)	11
			6	47	50	0	0	49	50 (**4**), 50 (**2**)	7
			7	49	55	0	0	49	52 (**4**), 49 (**2**)	11
			8	54	59	0	0	49	54 (**4**), 46 (**2**)	5
			10	59	66	0	0	50	55 (**4**), 45 (**2**)	7
			12	65	79	0	0	41	64 (**4**), 36 (**2**)	8
			24	83	98	0	0	0	100 (**4**), 0 (**2**)	3

[a] *Protocol A* , [b] *Protocol B*

Table SI-2. ***Continued***

Entry	Solvent, Temp	Promoter	Time (h)	Conversion caculated by signal integrations					% Conversion Avg.	Δ%
				Chloroaminal (**4b**)		Hemiaminal (**3**)		CBz-NH_2 (**2**)		
				$^{\alpha}H$	CH_2	$^{\alpha}H$	CH_2	CH_2		
5[b]	$CHCl_3$, RT	AcCl	0	-	-	-	-	100	100 (**2**)	0
			1	-	-	10	10	90	10 (**3**), 90 (**2**)	9
			2	-	-	20	10	85	15 (**3**), 85 (**2**)	8
			3	-	-	32	28	70	30 (**3**), 70 (**2**)	11
			4	-	-	26	26	74	26 (**3**), 74 (**2**)	5
			5			48	27	63	37 (**3**), 63 (**2**)	0
			7	3	4	53	58	41	3 (**4**), 56 (**3**), 41 (**2**)	9
			24	32	32	64	64	7	32 (**4**), 64 (**3**), 7 (**2**)	9
			28	46	56	50	50	0	50 (**4**), 50 (**3**), 0 (**2**)	14
			38	39	47	47	65	0	43 (**4**), 56 (**3**), 0 (**2**)	0
			48	56	69	40	41	0	62 (**4**), 40 (**3**), 0 (**2**)	5
6[b]	$CHCl_3$, 60 °C	AcCl	0	-	-	-	-	100	100 (**2**)	0
			1	-	-	63	60	38	62 (**3**), 38 (**2**)	8
			2	16	22	67	64	15	19 (**4**), 66 (**3**), 15 (**2**)	6
			3	61	56	35	40	3	59 (**4**), 37 (**3**), 3 (**2**)	5
			4	42	54	45	53	3	48 (**4**), 49 (**3**), 3 (**2**)	11
			5	59	66	31	37	3	63 (**4**), 34 (**3**), 3 (**2**)	12
			7	81	98	8	13	0	90 (**4**), 10(**3**), 0 (**2**)	18
			9	87	100	5	7	0	94 (**4**), 6 (**3**), 0 (**2**)	15
			11	100	100	0	0	0	100 (**4**), 0(**3**), 0 (**2**)	8
7[b]	$CHCl_3$, RT	$(CO)_2Cl_2$	0	-	-	-	-	100	100 (**2**)	0
			1	9	16	76	65	16	13 (**4**), 70 (**3**), 16 (**2**)	1
			2	14	24	73	60	12	19 (**4**), 67 (**3**), 12 (**2**)	2
			4	72	72	26	28	0	72 (**4**), 27 (**3**), 0 (**2**)	1
			15	84	82	16	17	0	83 (**4**), 17 (**3**), 0 (**2**)	5
			18	95	92	4	5	0	94 (**4**), 5 (**3**), 0 (**2**)	4

[a] *Protocol A* , [b] *Protocol B*

Table SI-2. ***Continued***

Entry	Solvent, Temp	Promoter	Time (h)	Conversion calculated by signal integrations			% Conversion Avg.	AcOH (mol%)	AcBr (mol%)	Δ%
				Bromoaminal **4c**		CBz-NH_2 (**2**)				
				αH	CH_2					
8[a]	$CDCl_3$, RT	AcBr	0	4	5	95	5 (**4**), 95(**2**)	36	269	9
			0.25	7	12	90	10 (**4**), 90 (**2**)	71	237	12
			0.5	26	18	78	22 (**4**), 78 (**2**)	73	240	15
			0.75	35	28	69	31 (**4**), 69 (**2**)	91	227	16
			1	44	38	59	41 (**4**), 59 (**2**)	87	212	5
			1.25	39	42	58	42 (**4**), 58 (**2**)	94	216	14
			1.5	53	51	48	52 (**4**), 48 (**2**)	100	202	8
			1.75	58	64	39	61 (**4**), 39 (**2**)	105	186	19
			2	66	68	33	67 (**4**), 33 (**2**)	127	168	6
			2.15	67	70	31	69 (**4**), 31 (**2**)	134	177	13
			2.5	69	73	29	71 (**4**), 29 (**2**)	138	179	14
			2.75	74	75	25	75 (**4**), 25 (**2**)	166	149	12
			3	76	79	22	78 (**4**), 22 (**2**)	152	169	13
			3.25	80	80	20	80 (**4**), 20 (**2**)	162	157	13
			3.5	81	82	19	81 (**4**), 19 (**2**)	165	160	14
			4	81	86	16	84 (**4**), 16 (**2**)	164	152	13
			5.5	91	91	9	91 (**4**), 9 (**2**)	165	155	16
			6.5	100	100	0	100 (**4**)	183	111	9

Table SI-2. *Continued*

Entry	Solvent, Temp	Promoter	Time (h)	Conversion calculated by signal integrations			% Conversion Avg.	Δ%
				Bromoaminal **4c**		CBz-NH_2 (**2**)		
				αH	**CH_2**			
9[a]	$CDCl_3$, RT	TMSBr	0	14	11	87	13 (**4**), 87(**2**)	13
			0.25	22	23	77	23 (**4**), 77(**2**)	13
			0.5	40	34	37	37 (**4**), 63 (**2**)	10
			0.75	43	40	58	42 (**4**), 58 (**2**)	9
			1	47	55	50	50 (**4**), 50 (**2**)	12
			1.5	74	74	26	74 (**4**), 26 (**2**)	8
			2	81	86	17	83 (**4**), 17 (**2**)	12
			2.5	83	93	12	88 (**4**), 12 (**2**)	12
			3	80	98	11	89 (**4**), 11 (**2**)	11
			3.5	82	100	8	92 (**4**), 8 (**2**)	9
			4	100	100	0	100 (**4**), 0 (**2**)	13

[a] *Protocol A* , [b] *Protocol B*

In the case of acetyl chloride as an activator at room temperature, benzyl carbamate **2** was rapidly consumed, generating the intermediate hemiaminal **3** (Fig. SI-1). Hemiaminal **3** formation reached a maximum concentration at ~25 h and then plateaued over time with concomitant formation of the chloroaminal **4b**. This significant amount of hemiaminal accumulating ~60% over time suggests that the rate determining step is the formation of the iminium.

AcCl/AcOH, RT: Table SI-2, entry 1

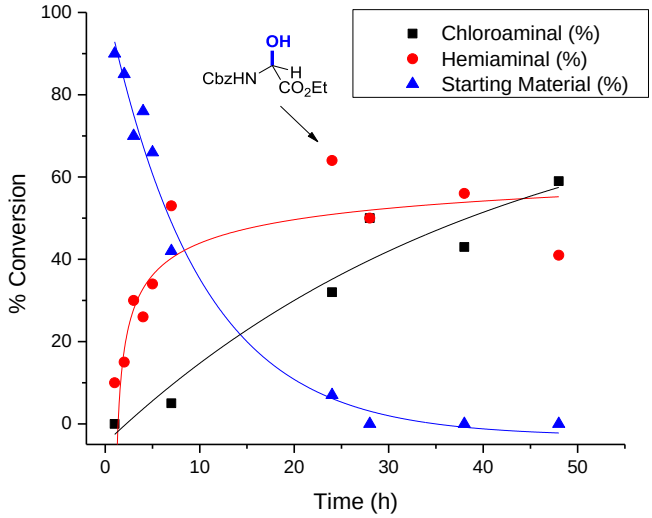

Figure SI-1: Kinetic data for the synthesis of **4b** in one-pot using AcCl as promoter.

When the acetyl chloride was used as an activator at higher temperature (60 °C), benzyl carbamate **2** was consumed rapidly, generating hemiaminal **3** as the major intermediate (Fig. SI-2). The formation of hemiaminal **3** reached a maximum concentration at ~115 min and consumed overtime with concomitant formation of the chloroaminal **4b**. At higher temperature there was shift in maxima for hemiaminal formation suggesting that the formation of iminium from the hemiaminal is faster at higher temperature, which is also proposed to be the rate-determining step for the reaction.

AcCl/AcOH, 60 °C: Table SI-2, entry 2

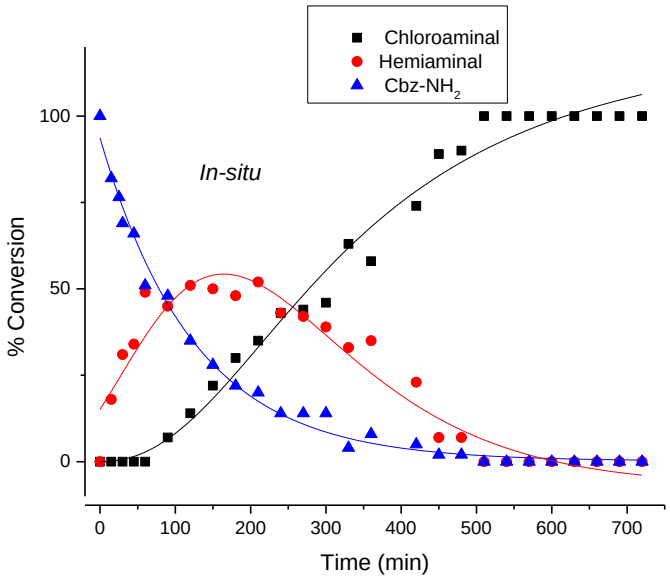

Figure SI-2: Kinetic data for the synthesis of **4b** in one-pot using AcCl as promoter at 60 °C.

However, when $SiCl_4$ was used an activator, benzyl carbamate **2** was consumed concomitantly to the formation of product **4b**. Reaction's profiling were achieved by an *in-situ* NMR analysis of aliquots in $CDCl_3$:CD_3CN solvent mixture (Figure SI-3). The conversion data are plotted and best fitted using OriginPro 9.0 software. The intermediate hemiaminal **3** was not observed over time, suggesting that $SiCl_4$ is a very reactive promoter to accelerate the formation and trapping of the iminium intermediate (no accumulation of **3** was observed)**.**

$SiCl_4$, 35 °C: Table SI-2, entry 3

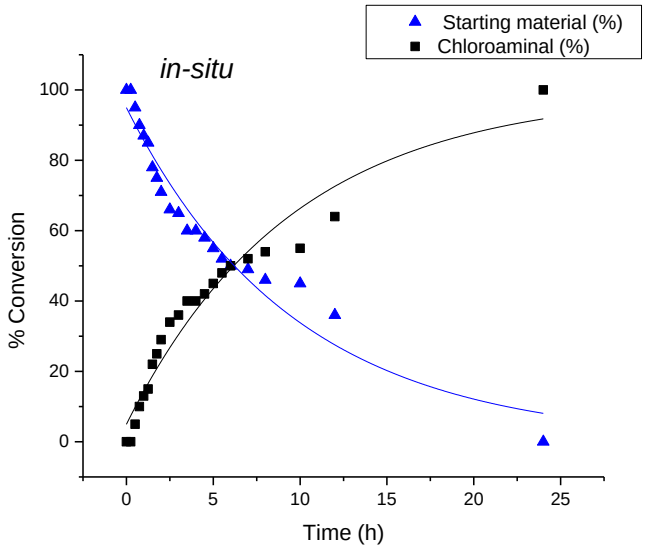

Figure SI-3*:* Kinetic data for the synthesis of **4b** in one-pot using $SiCl_4$ as promoter

$SOCl_2$, RT: Table SI-2, entry 4

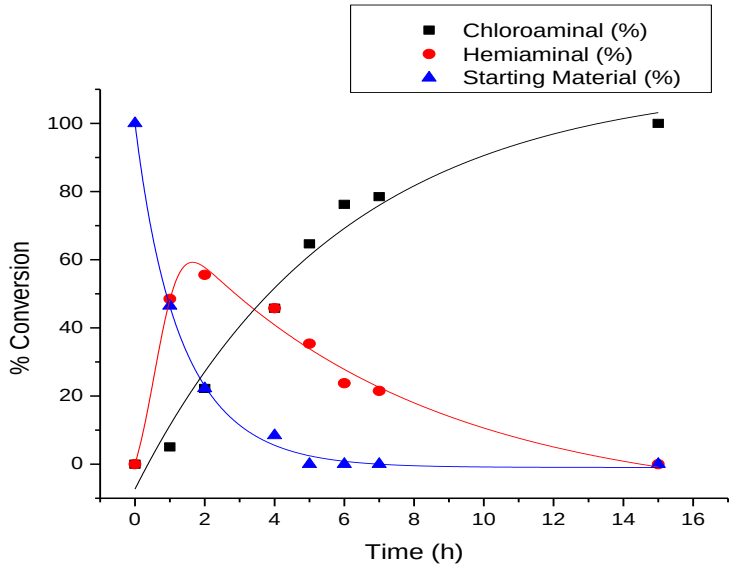

Figure SI-4*:* Kinetic data for the synthesis of **4b** in one-pot using $SOCl_2$ as promoter.

In the presence of thionyl chloride as activator, the reactions' kinetics presented similar profiles at RT vs higher temperature (60 °C) as shown in Figure SI-4 and Figure SI-5. In both cases, the starting material Cbz-carbamate **2** disappearance followed an exponential decay, the intermediate hemiaminal **3** formation reached maximum around ~2 h with 60% and 50% conversion, respectively. The reaction seemed to be completed in 6 h at 60 °C while the full conversion happened at 15 h for the reaction at RT.

$SOCl_2$, 60 °C: Table SI-2, entry 5

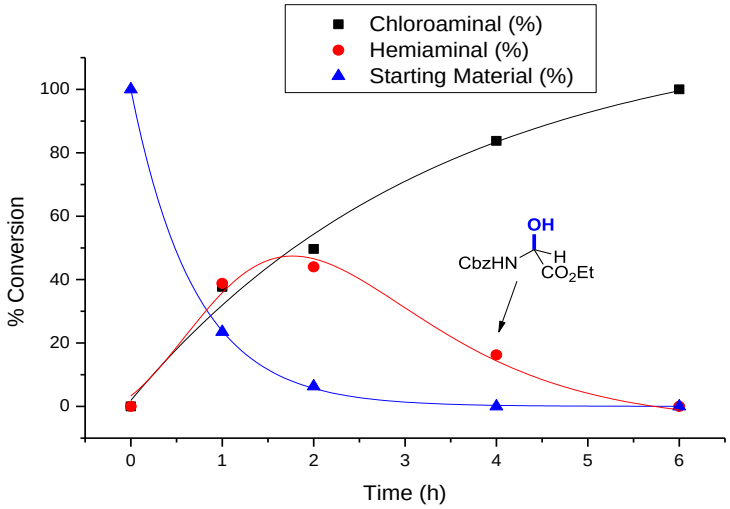

Figure SI-5*:* Kinetic data for the synthesis of **4b** in one-pot using $SOCl_2$ as promoter.

While using the less reactive TMSCl as activator, the reaction seemed slow compared to other activators (Figure 6). After 60 h, the reaction did not proceed to full conversion to the desired chloroaminal **4b**. The concentration in hemiaminal **3** was high and reached a maximum concentration at ~15 h. The accumulation of the hemiaminal **3** over a long period of time suggests that the formation of the iminium and trapping by the chloride anion is the rate-determining step.

TMSCl, RT: Table SI-2, entry 6

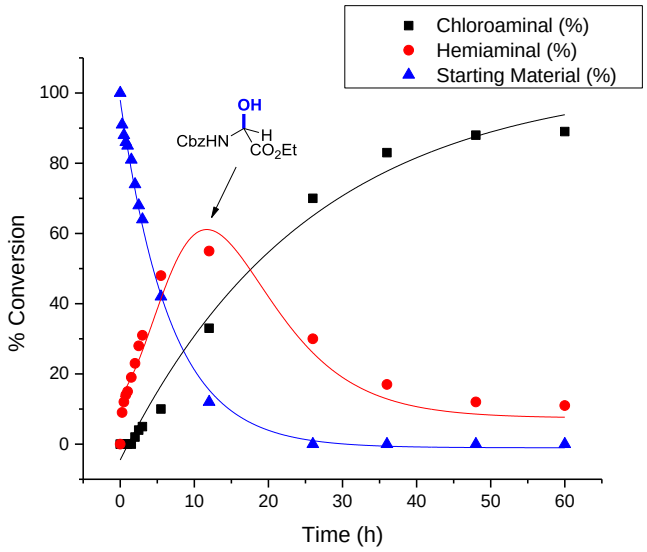

In the case of oxalyl chloride as activator at room temperature, benzyl carbamate **2** was consumed rapidly, generating intermediate hemiaminal **3** (Fig. SI-7). Hemiaminal **3** formation reached a maximum concentration at a very early stage of the reaction ~2 h with ~80% conversion and then disappeared with the concomitant formation of the chloroaminal **4b**.

$(CO)_2Cl_2$, RT: Table SI-2, entry 7

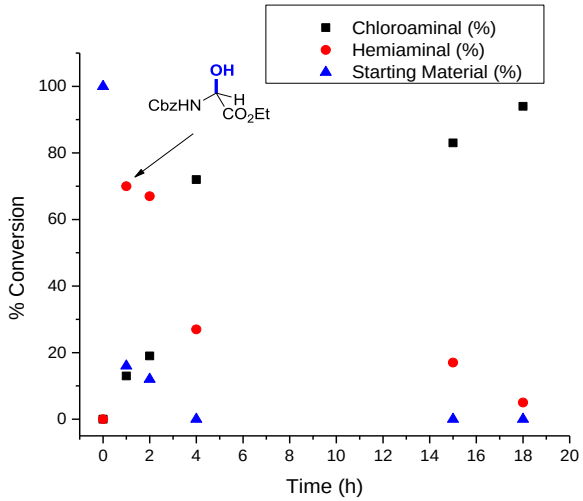

Figure SI-7: Kinetic data for the synthesis of **4b** in one-pot using $(CO)_2Cl_2$ as promoter.

When the promoters of deoxyhalogenation were switched to brominating reagents such as AcBr and TMSBr, intermediate hemiaminal **3** was not observed (Figures SI-8 and SI-9). In both cases (AcBr and TMSBr), the disappearance of Cbz-carbamate **2** followed an exponential decay, leading to a quasi-full conversion in **4c** in 6.5 h and 4 h, respectively. The lower pKa of HBr and the enhanced nucleophilicity of the bromide ion might be two separate effects that contribute to a rapid formation of the iminium intermediate and its *in situ* trapping into bromoaminal **4c**.

AcBr, RT: Table SI-2, entry 8

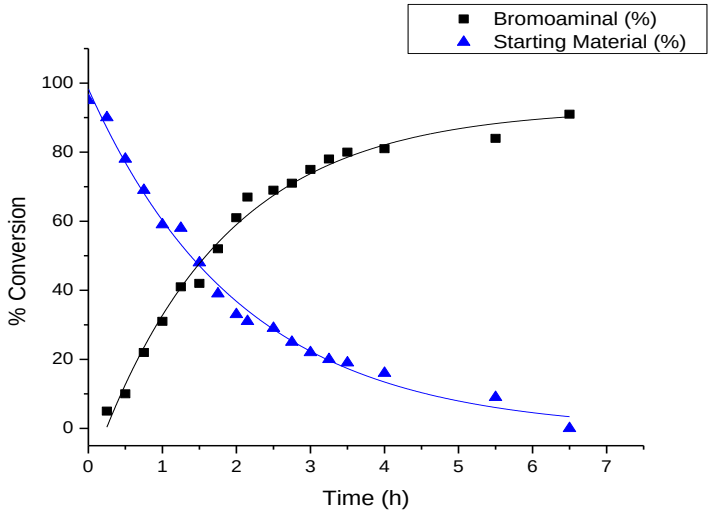

Figure SI-8*:* Kinetic data for the synthesis of **4c** ester in-one pot using AcBr as promoter.

TMSBr, RT: Table SI-2, entry 9

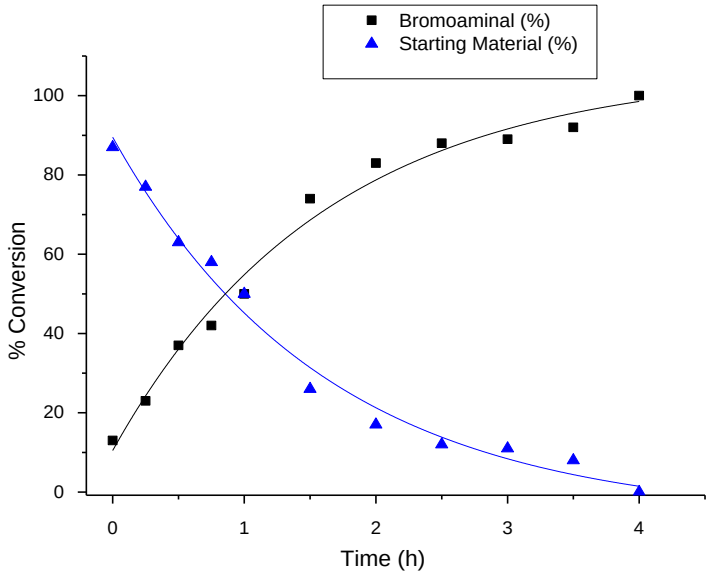

Figure SI-9: Kinetic data for the synthesis of **4c** in one-pot using TMSBr as promoter.

Conclusion.

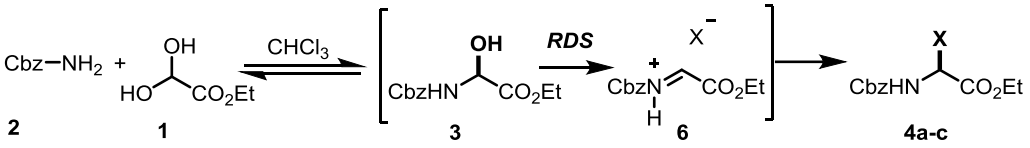

We examined several reagents to enable the cascade of condensation and deoxyhalogenation to occur in the same reaction vessel (one-pot). Reactions were monitored by ^{1}H NMR to examine the potential differences in kinetic profiles. The results suggest that the rate-determining step of the cascade of events is in most cases the halogenation of α-hydroxyglycine **3** (hemiaminal) to the corresponding haloglycine **4a-c**. As shown above, in Figures SI-1 to SI-9, the amount of intermediate **3** building-up was different in each reaction, which seemed to correspond to the strength of the halogenation reagent. Given that reactions involving the same ion (*e.g.* bromide) proceeded at different rates, the rate-determining step is likely glycinyl iminium **6** ion formation. Reactions carried with brominating reagents were found to be much faster due to the higher acidity of HBr and the enhanced nucleophilicity of the bromide ion. These brominating agents formed and trapped the glycinyl iminium **6** at much faster rates as exemplified by the synthesis of α-bromoglycine ester **4c** in less than 15 minutes at -20 °C (see Table SI-2, entry 8).

II. Autocatalysis-like mechanism mediated by AcCl and AcOH (cat.) for the synthesis of α-chloroglycine ester 4b

α-Chloroglycine **4b** can be synthesized at RT or 60 °C with AcOH/AcCl in 48 h to 11 h respectively. In the case of AcOH (cat.) /AcCl as a combination of reaction promoters, the starting material Cbz-carbamate **2** disappearance followed an exponential decay, but the unusual shape (sigmoid) for the plot of product **4b** formation overtime suggested a complex reaction mechanism (Figure SI-2). Therefore, we decided to study this reaction with AcOH(cat.)/AcCl (Table SI-2, entry 1) in detail to gain more mechanistic insight (Figure SI-10A). The reaction was performed in flamed dry scintillation vials (1 drum) equipped with a stirring bar and placed under an inert atmosphere of argon. The vial was initially charged with benzyl carbamate (76 mg, 0.5 mmol, 1.0 eq.), internal standard mesitylene (60 mg, 0.5 mmol, 1.0 eq.) in freshly prepared $CDCl_3$ (5 mL passed through a plug of neutral alumina ~1.0 g) followed by ethyl glyoxylate (*c.a.*50% in toluene, 145 µL, 0.6 mmol, 1.2 eq.) and finally the promoter AcCl (2.5 eq.). The reaction was carried at 60 °C and at specific times (see Table SI-3), an aliquot of the reaction mixture (150 µL) was transferred using a dry syringe to a flame dried NMR tube and CD_3CN (300 µL) was added to complete the volume of 450 µL. Note: CD_3CN was selected as cosolvent for the 1H NMR because signals are better splitted and the reaction kinetics are slow down in comparison to $CDCl_3$. The progress of the reaction was monitored via ^1H NMR analysis of the aliquots in a $CDCl_3$-CD_3CN mixture (2:1 ratio).

The slow formation of product α-chloroglycine ester **4b** in the initial 100 minutes corresponds to a timeframe in which a glyoxylate dehydration occurs (step 1) with the formation of a plausible oxonium which further initiates the condensation (step 2) to the hemiaminal intermediate **3**. The maximum conversion in hemiaminal **3** can be seen at ~150 minutes suggesting that the rate-determining step of the reaction is the iminium **6** formation. From there, by-product AcOH and product **4b** formation followed similar kinetics with an acceleration and a deceleration phase typical of an autocatalysis-like mechanism. The rate profile for the by-product AcOH (autocatalyst) was plotted (d[AcOH]/dt, see Figure SI-10b) and confirmed that the acceleration phase proceeded from 100 to 200 minutes at which time the rate of formation in **4b** is also maximal before decelerating toward the end of the reaction as shown in Figure SI-10b-c. The fact that similar kinetic profiles (autocatalysis-like) were not observed in other reactions (Table SI-2, entries 2-12) suggested that the rate limiting step shifted due to change in promoter strength.

Table SI-3

Entry	Solvent, Temperature	Promoter	Time (h)	Conversion calculated by signal integrations					Conversion Avg (%)	AcOH (mol%)	Δ%
				Chloroaminal (**4**)		Hemiaminal (**3**)		CBz-NH_2 (**2**)			
				$^{\alpha}H$	CH_2	$^{\alpha}H$	CH_2	CH_2			
1	$CDCl_3$, 60 °C	AcCl	0	-	-	-	-	100	100 (**2**)	13	10
			0.25	-	-	19	17	82	18 (**3**), 82 (**2**)	26	9
			0.5	-	-	34	28	69	31 (**3**), 69 (**2**)	25	7
			0.75	-	-	37	32	66	34 (**3**), 66 (**2**)	37	8
			1	-	-	49	49	51	49 (**3**), 51 (**2**)	51	7
			1.5	7	8	46	43	51	7 (**4**), 45 (**3**), 48 (**2**)	38	11
			2	14	14	53	48	35	14 (**4**), 51 (**3**), 35 (**2**)	47	9
			2.5	20	23	50	50	28	22 (**4**), 50 (**3**), 28 (**2**)	51	4
			3	27	33	48	48	22	30 (**4**), 48 (**3**), 22 (**2**)	56	8
			3.5	34	36	50	53	20	35 (**4**), 52 (**3**), 20 (**2**)	70	8
			4	41	46	44	43	14	43 (**4**), 43 (**3**), 14 (**2**)	82	6
			4.5	41	42	44	44	14	44 (**4**), 42 (**3**), 14 (**2**)	84	6
			5	42	50	38	40	15	46 (**4**), 39 (**3**), 14 (**2**)	90	2
			5.5	57	68	29	36	4	63 (**4**), 33 (**3**), 4 (**2**)	104	10
			6	51	63	34	37	8	58 (**4**), 35 (**3**), 8 (**2**)	113	9
			7	72	77	23	23	5	74 (**4**), 23 (**3**), 5 (**2**)	118	6
			7.5	89	89	6	7	2	89 (**4**), 7 (**3**), 2 (**2**)	115	7
			8	92	88	7	6	2	90 (**4**), 7 (**3**), 2 (**2**)	121	7
			8.5	100	100	0	0	0	100 (**4**), 0 (**3**), 0 (**2**)	117	9
			9	100	100	0	0	0	100 (**4**), 0 (**3**), 0 (**2**)	118	6
			9.5	100	100	0	0	0	100 (**4**), 0 (**3**), 0 (**2**)	134	6
			10	100	100	0	0	0	100 (**4**), 0 (**3**), 0 (**2**)	146	7
			10.5	100	100	0	0	0	100 (**4**), 0 (**3**), 0 (**2**)	164	9
			11	100	100	0	0	0	100 (**4**), 0 (**3**), 0 (**2**)	213	7
			11.5	100	100	0	0	0	100 (**4**), 0 (**3**), 0 (**2**)	214	7

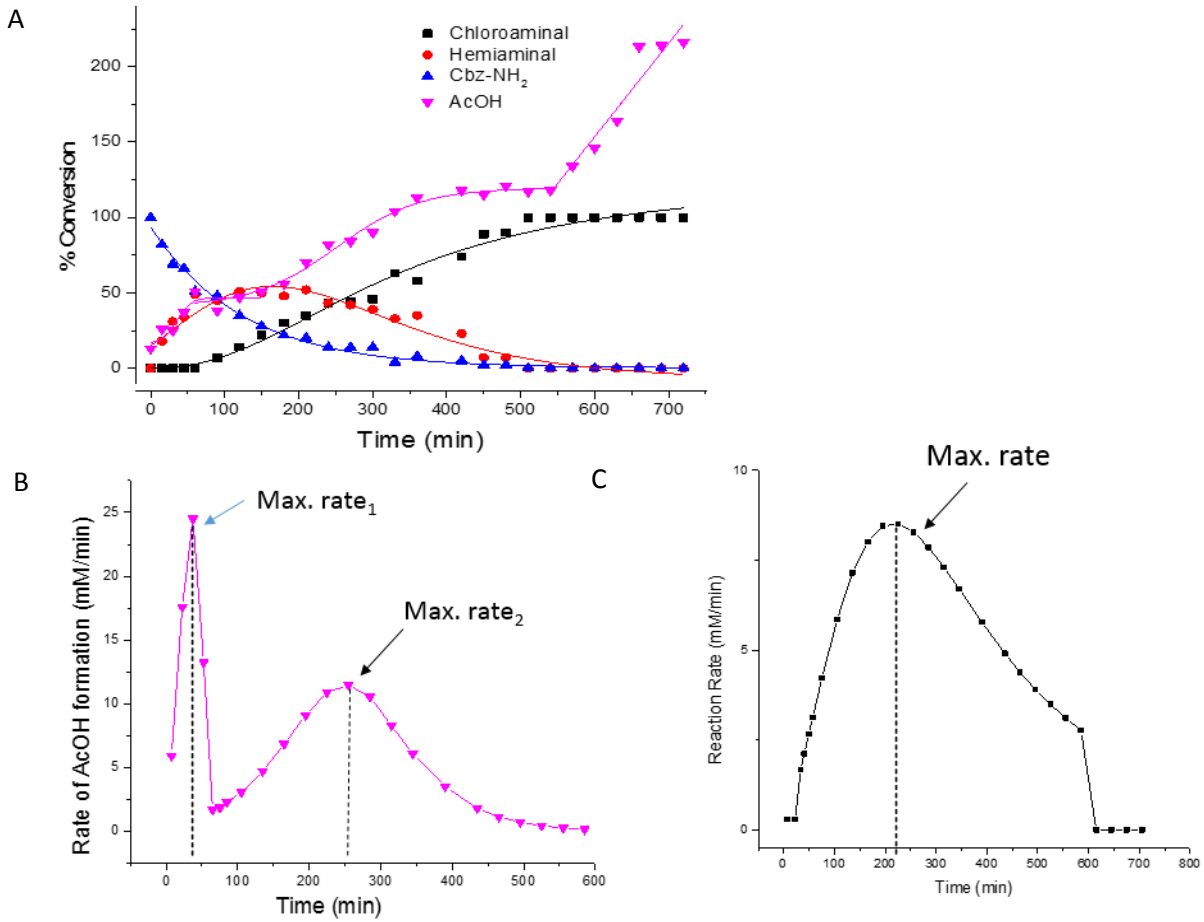

Time (Min)	Rate(mM/min)
7.5	0.30
22.5	0.30
33	1.67
40.5	2.12
49.5	2.67
57	3.13
75	4.22
105	5.85
135	7.15
165	8.01
195	8.45
225	8.51
255	8.29
285	7.86
315	7.31
345	6.70
390	5.78
435	4.91
465	4.38
495	3.91
525	3.49
555	3.11
585	2.77
615	0
645	0
675	0
705	0

Fig. SI-10: **Panel A:** Kinetic profile for the synthesis of **4b** using AcOH (cat.)/AcCl. **Panel B**: Rate in AcOH formation with 2 successive acceleration deceleration phases suggesting an autocatalysis-like mechanism. **Panel C:** Rate in α-haloglycines **4b** formation (reaction rate).

III. Reactivity of α-Haloglycine Esters 4a-c: Friedel–Crafts and Mannich Reactions

a) Competitive experiments for the Friedel–Crafts reaction:

In the following experiments, the 3 α-haloglycines (X= F, Cl, and Br) were reacted together with a neutral π-nucleophile (N-methyl indole). On one hand, the uncatalyzed reaction have shown that the α-chloroglycine **4b** is the most reactive substrate, but under thiourea-catalysis the α-bromoglycine **4c** was found to react faster to deliver the desired Friedel–Crafts product **7**. Each time when the conversion in chloride is important, a bromide-chloride exchange is likely occurring which complicates slightly our assessment.

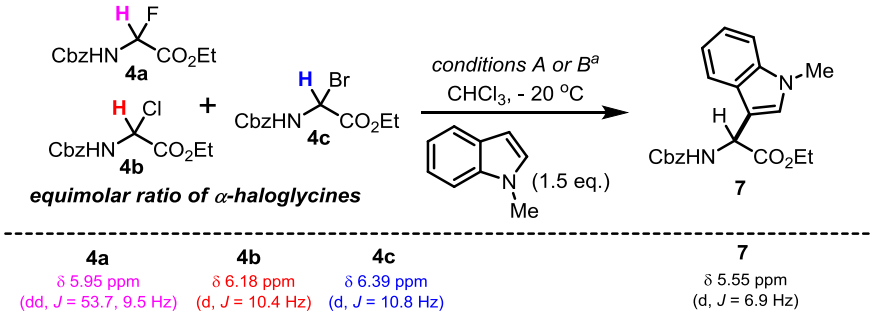

Protocol: All reactions were performed in flamed dry scintillation vials (1 drum) equipped with a stirring bar and placed under an inert atmosphere of argon. The vial was initially charged with an equimolar mixture of the 3 α-haloglycines **4a-c** (0.5 mmol, 1.0 eq.), mesitylene as the internal standard (60 mg, 1.0 eq.) in freshly distilled $CHCl_3$ (5 mL) at -78 °C, followed by N-methyl Indole (94 µL, 0.8 mmol, 1.5 eq.), condition A (no catalyst), and finally with the Schreiner thiourea catalyst (25 mg, 10 mol%, 0.1 eq.) with respect to condition B. The reactions were then stirred at -20 °C for several hours and aliquots were taken for reaction monitoring by ^{1}H NMR.

Recording data points to assess the reaction course: At specific times (see Tables SI-3 to SI-5), an aliquot of the reaction mixture (150 µL) was transferred using a dry syringe to a flame dried NMR tube, and CD_3CN (300 µL) was added to the sample (450 µL total volume per tube) to help splitting several signals in the ^{1}H NMR. Then, the NMR tube was frozen to -78°C for a couple of minutes to allow transportation to the NMR facility. The temperature of the NMR tube was raised back to -20 °C before the ^{1}H NMR spectrum was recorded.

Note: The experiments were run in triplicate for reproducibility and the measurement averages are reported in Tables SI-4 to SI-6.

Table SI-4: Reactivity of the α-fluoroglycine **4a**

Uncatalyzed reaction: % Consumption of α-fluoroglycine **4a**									
Time (min)	15	30	60	90	150	210	360	480	600
Exp 1	0	13	8	21	45	50	61		
Exp 2	19	10	29	6	13	23	0	16	32
Exp 3	23	23	26	23	29	23	39	35	35
Average	**14**	**15.3**	**21**	**16.7**	**29**	**32**	**33.3**	**25.5**	**33.5**
Thiourea-Catalyzed reaction**:** % Consumption of α-fluoroglycine **4a**									
Time (min)	15	30	60	90	150	210	360	480	600
Exp 1	41	13	24	23	34	26	39		
Exp 2	0	0	0	0	0	3	0	0	35
Exp 3	29	32	39	26	39	32	35	32	10
Average	**23.3**	**15**	**21**	**16.3**	**24.3**	**20.3**	**24.7**	**16**	**22.5**

Table SI-5: Reactivity of the α-chloroglycine **4b**

Uncatalyzed reaction: % Consumption of α-chloroglycine **4b**									
Time(min)	15	30	60	90	150	210	360	480	600
Exp 1	33	41	56	41	37	44	48		
Exp 2	34	28	66	72	53	38	13	53	28
Exp 3	43	47	50	40	47	40	80	53	63
Average	**36.7**	**38.7**	**57.3**	**51**	**45.7**	**40.7**	**47**	**53**	**45.5**
Thiourea-Catalyzed reaction**:** % Consumption of α-chloroglycine **4b**									
Time(min)	15	30	60	90	150	210	360	480	600
Exp 1	44	42	33	63	44	48	81		
Exp 2	13	34	25	34	41	53	34	19	31
Exp 3	47	60	67	53	50	53	83	67	47
Average	**34.7**	**45.3**	**41.7**	**50**	**45**	**51.3**	**66**	**43**	**39**

Table SI-6: Reactivity of the α-bromoglycine **4c**

Uncatalyzed reaction: % Consumption of α-bromoglycine **4c**									
Time(min)	15	30	60	90	150	210	360	480	600
Exp 1	0	0	0	17	29	49	70		
Exp 2	5	11	16	16	19	38	27	49	76
Exp 3	18	23	23	36	46	46	62	74	79
Average	**7.6**	**11.3**	**13**	**23**	**31.3**	**44.3**	**53**	**61.5**	**77.5**
Thiourea-Catalyzed reaction**:** % Consumption of α-bromoglycine **4c**									
Time(min)	15	30	60	90	150	210	360	480	600
Exp 1	14	31	43	57	51	66	69		
Exp 2	16	54	35	41	49	62	57	54	76
Exp 3	49	59	67	72	77	85	85	92	100
Average	**26.3**	**48**	**48.5**	**56.7**	**59**	**71**	**70.3**	**73**	**88**

Uncatalyzed reaction:

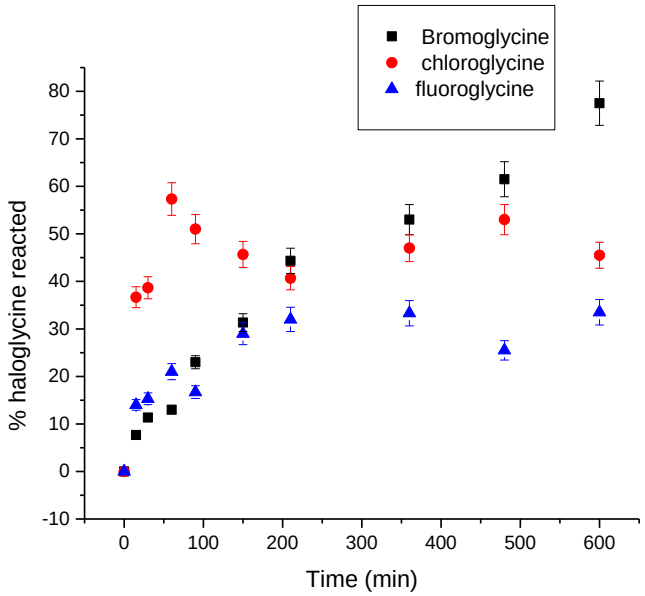

Figure SI-11. Direct comparison of reactivity between α–haloglycines **4a**, **4b** and **4c**

Thiourea-Catalyzed reaction:

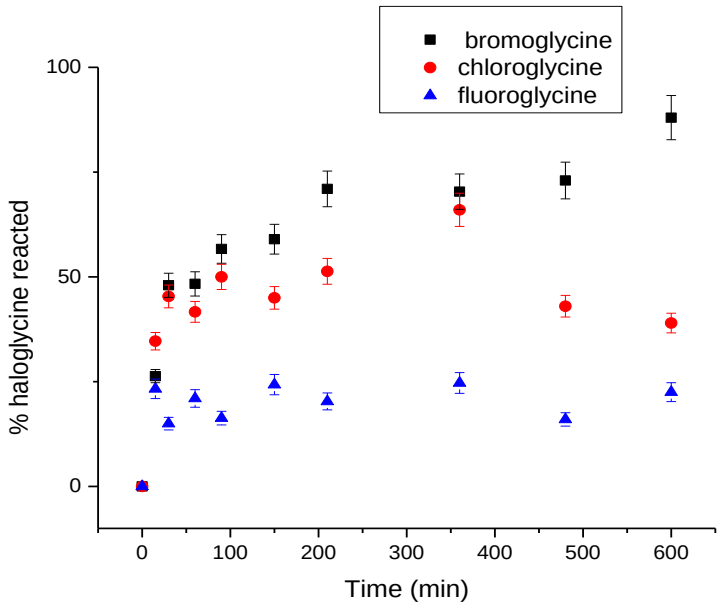

Figure SI-12. Direct comparison of Reactivity between α–haloglycines **4a**, **4b** and **4c** in presence of the Schreiner thiourea catalyst.

In conclusion from the above competitive experiments (cat. vs uncat. reactions), we observed:

1. α-Fluoroglycine **4a** reacted in an uncontrolled manner with the borosilicate glass and further experiments (not shown) in PTFE vessel demonstrated that 4a did not react with N-methyl Indole in a Friedel-Crafts reaction.

2. For α-chloroglycine **4b**, the consumption is rapid and it follows similar trends with or without the presence of the hydrogen-bond donor thiourea catalyst $\mathbf{T_A}$. This suggests that the effect of the Schreiner catalyst on this substrate is limited. When ~50% of α-chloroglycine **4b** is consumed (~ 150 mins), the regeneration of **4b** is observed, which presumably occurs due to an ion exchange between the HCl (formed) and the α-bromoglycine **4c** substrate.

3. In the uncatalyzed reaction, α-bromoglycine **4c** reacts quite slowly and a major conversion is only observed after 150 mins, which does not appear to correlate to the product **7** formation (see above corresponding to the ion exchange). More interestingly, in the reactions catalyzed by the hydrogen-bond donor thiourea $\mathbf{T_A}$, the reactivity of α-bromoglycine **4c** is drastically enhanced (> 30 mins), suggesting that a bromide-binding mechanism might be operating, thus facilitating the N-methyl Indole addition in the second step: $S_N2(C+)$ (Figure SI-13).

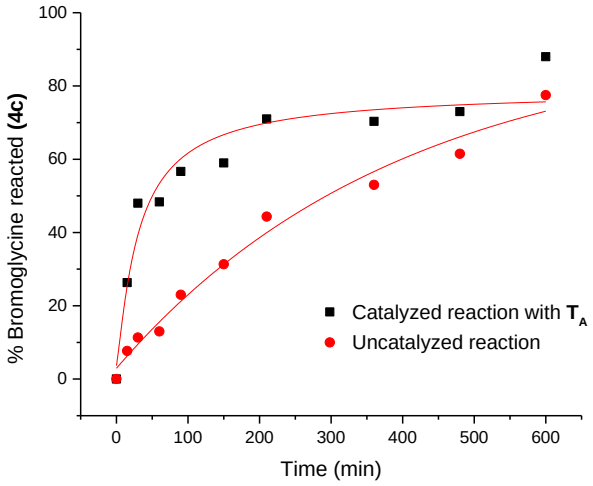

Figure SI-13. Comparison of the catalyzed vs uncatalyzed reactions with α-bromoglycine **4c.**

b) Catalyzed and Uncatalyzed Mannich Reactions:

To confirm these initial results, we further studied the Mannich reactions of α-chloroglycine **4b** and α-bromoglycine **4c** in individual reaction vessels to avoid any undesirable ion-return effect and therefore being able to compare the thiourea catalyst effect on these substrates. All reactions were performed in flamed dry NMR tube under an inert atmosphere of argon in CD_2Cl_2. The *in situ* NMR data were recorded on a Varian 400 MHz at 0 °C every 20 minutes after stirring continuously for 2 mins using a Vortex lab-mixer in-between each data point. At first, the kinetic profiling of the Mannich reaction between α-chloroglycine **4b** (1.0 eq.) and the 1,3-dicarbonyl nucleophile (2.0 eq.) was achieved in CD_2Cl_2 at 0 °C with and without the presence of the enantiopure thiourea-catalyst $\mathbf{T_B}$ (Takemoto thiourea) using 25 mol% of NEt_3 and one bead (~20 mg) of 4Å MS in an NMR tube. The catalytic reactions have been achieved under similar conditions to the enantioselective transformation reported previously by Jacobsen and Roche (at – 30 °C). While the uncatalyzed reaction did not proceed during the initial 6 h (<9 % conversion), the reaction catalyzed by $\mathbf{T_B}$ produced ~40% of desired product **8** over the same course of time.

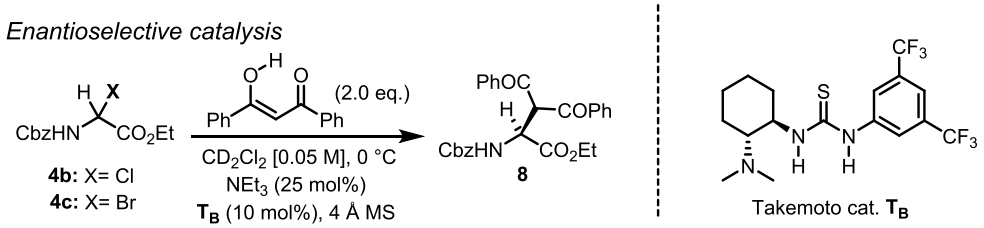

Furthermore, the reactions proved to be catalyzed by the Takemoto's tertiary aminothiourea $\mathbf{T_B}$ at -20°C leading to about 20% yield from α-bromoglycine **4c** in 6 h compare to uncatalyzed reaction which gives only 7% yield. However raising the temperature to 0°C the yield of the reaction does not seems to improve. From the reactions profile, it appears that catalyst $\mathbf{T_B}$ might be rapidly quenched by the formation of HBr salt under the reaction conditions. Nonetheless, catalyst $\mathbf{T_B}$ displayed a markedly enhanced reactivity toward **4b**, affording high conversion in product **7** as previously reported (conv. > 35% at 2 hours). Note: Without the 2 mins stirring in between each data point, the catalyzed reaction do not proceed and a yellow solution was observed at the MS bead proximity which might imply that the bead is important to regenerate the catalyst and drive the reaction advancement (possible in-and-out of Net2-HCl to sequester the HCl generated and/or also form a sodium enolate of the 1,3-dicarbonyl pronucleophile).

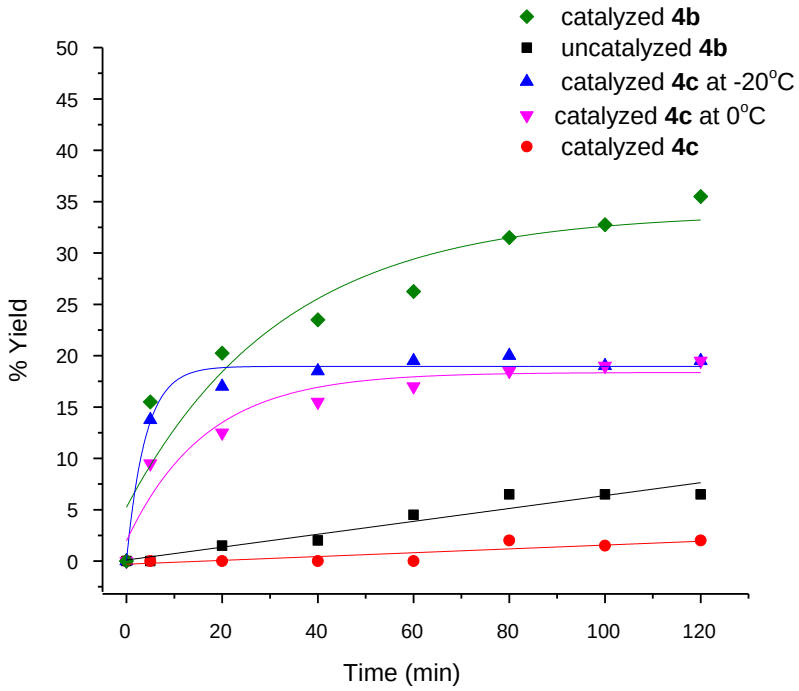

Figure SI-14. Comparison of catalyzed vs uncatalyzed reactions with α-chloro **4b** and α-bromoglycine **4c.**

In Summary, we investigated the kinetics of the Mannich reactions between α-chloroglycine **4b** and α-bromoglycine **4c** with or without thiourea catalyst $\mathbf{T_B}$. Initial rate constants (k_{obs}) were calculated in all cases (entries 1-4) using the first 2 data points.

Entry	Initial substrate concentration	$[\mathbf{Nu}]_0$	**Catalyst $\mathbf{T_B}$ (mol%)**	K_{obs} $[M^{-1}min^{-1}]^a$ (10^{-3})
1	$\mathbf{[4b]_0}$ = 0.05 M	0.01 M	10	31
2	$\mathbf{[4b]_0}$ = 0.05 M	0.01 M	0	0.75
3	$\mathbf{[4c]_0}$ = 0.05 M	0.01 M	10	19
4	$\mathbf{[4c]_0}$ = 0.05 M	0.01 M	0	0

[a]Conversions were calculated based on ^{1}H NMR using mesitylene as internal standard;

IV. Structural Study of the "Generalized" Anomeric Effect on α-Haloglycine Esters 4a-c

Hyperconjugative effects in the series of pyranosyl halides has been extensively studied and characterized by abnormal bond lengths. X-ray crystallographic data in Figures SI-15–17 highlight the bond elongation of the C(1)–X_{ax} which are commonly explained by the presence of an anomeric effect created by the hyperconjugation of the oxygen lone pair (n) electronic donation through space into the antibonding $\sigma^*_{(C-X)}$ orbital. [SI-1, SI-2, SI-3]

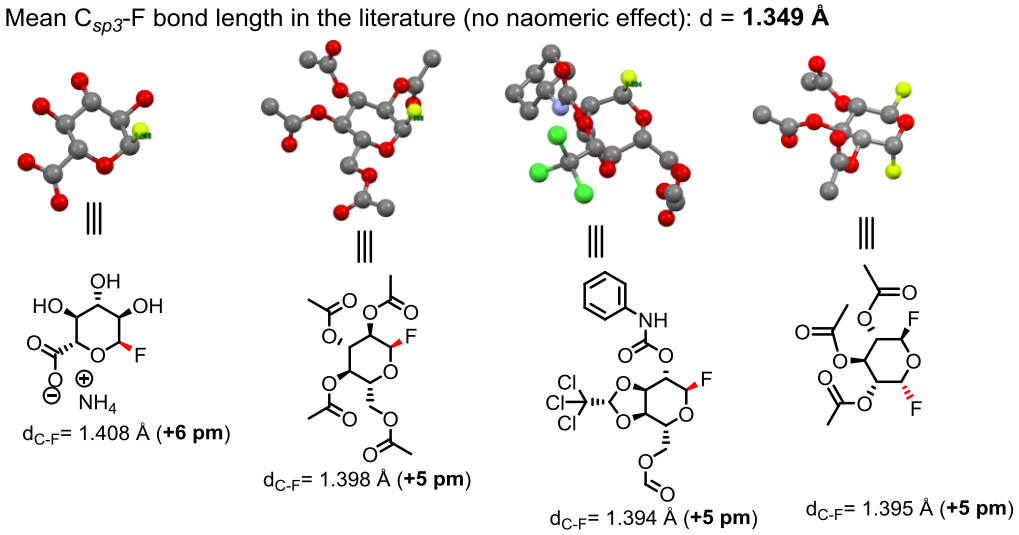

Figure SI-15. X-ray structures of several pyranoses containing and elongated C_{sp3}–F bond

[SI-1] For bond elongation of pyranosyl fluoride, see: (a) Reinke, H.; Rentsch, D.; Miethchen, R. *Carbohydr. Res.* **1996,** *281*, 293. (b) Dedola, S.; Hughes, D. L.; Field, R. A. *Acta Crystallogr., Sect. C: Cryst. Struct. Commun.* **2010,** *66*, o124. (c) Wilkinson, S. M.; Watson, M. A.; Willis, A. C.; McLeod, M. D. *J. Org. Chem.* **2011,** *76*, 1992. (d) Lee, S. S.; Greig, I. R.; Vocadlo, D. J.; McCarter, J. D.; Patrick, B. O.; Withers, S. G. *J. Am. Chem. Soc.* **2011,** *133*, 15826.

[SI-2] For bond elongation of pyranosyl chloride, see: (a) Lichtenthaler, F. W.; Rönninger, S.; Kreis, U. *Liebigs Ann. Chem.* **1990,** 1001. (b) Armishaw, O. A.; Cox, P. J.; Hassan, A. K.; Wardell, J. L. *J. Chem. Crystallogr.* **1996,** *26*, 701. (c) Lichtenthaler, F. W.; Sakakibara, T.; Oeser, E. *Carbohydr. Res.* **1977,** *59*, 47.

[SI-3] For bond elongation of pyranosyl bromide, see : (a) Doherty, R. M.; Stewart, J. M.; Benson, W. R.; Maienthal, M. M.; De Camp, W. H. *Carbohydr. Res.* **1983,** *116*, 150. (b) Praly, J.-P.; Brard, L.; Descotes, G.; Toupet, L. *Tetrahedron* **1989,** *45*, 4141. (c) Benz, A.; Immel, S.; Lichtenthaler, F. W. *Tetrahedron: Asymmetry* **2007,** *18*, 1108. (d) Hugenberg, V.; Frohlich, R.; Haufe, G. *Org. Biomol. Chem.* **2010,** *8*, 5682. (e) Mönch, B.; Gebert, A.; Emmerling, F.; Becker, R.; Nehls, I. *Carbohydr. Res.* **2012,** *352*, 186.

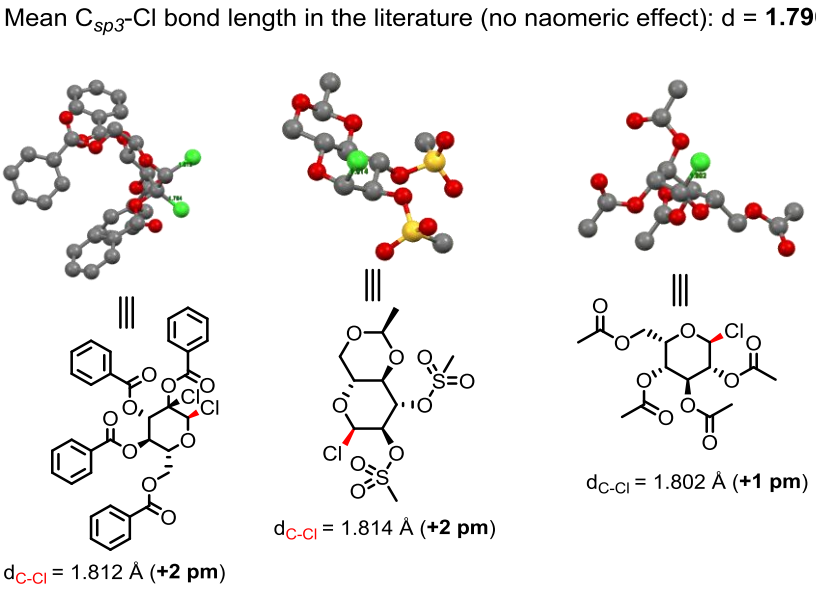

Figure SI-16. X-ray structures of several pyranoses containing an elongated C_{sp3}–Cl bond

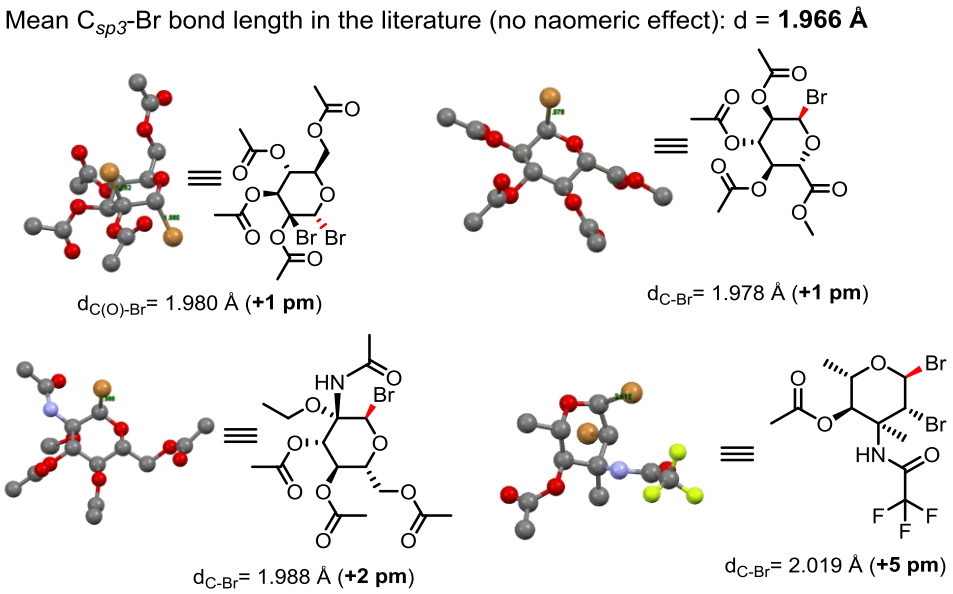

Figure SI-17. X-ray structures of several pyranoses containing an elongated C_{sp3}–Br bond

a) X-Ray Crystallographic Data for the N-Cbz α-Bromoglycine ester 4c

In a flame dried vial, approximately 50 mg of α-Bromoglycine ester **4c** were dissolved in 1 mL of toluene. Gentle heating was required to completely dissolve **4c**. The vial was sealed and wrapped in parafilm with a very small needle through the septum for slow evaporation and the vial was placed inside a desiccator to stand undisturbed for the crystallization to occur in 2 days.

Bond lengths: C_{sp3}-Br (C2-Br: 2.006 Å); C_{sp3}-N_{sp2} (C2-N: 1.406 Å); C_{sp3}-C_{sp2} (C2-C1: 1.516 Å);
Bond angles: Br-C2-N (112.1 º); Br-C2-C1 (105.3 º); Br-C2-H (109.8 º); N-C2-C1 (110.2 º)
Internal Hydrogen bond NH···O=COEt (weak: 2.491 Å)

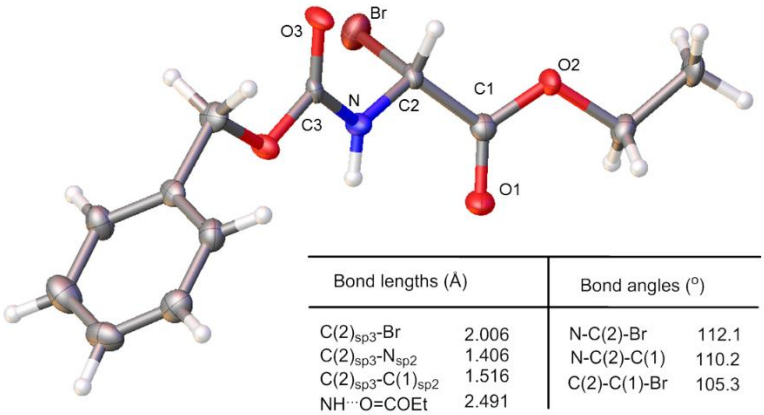

Bond lengths (Å)		Bond angles (º)	
$C(2)_{sp3}$-Br	2.006	N-C(2)-Br	112.1
$C(2)_{sp3}$-N_{sp2}	1.406	N-C(2)-C(1)	110.2
$C(2)_{sp3}$-$C(1)_{sp2}$	1.516	C(2)-C(1)-Br	105.3
NH···O=COEt	2.491		

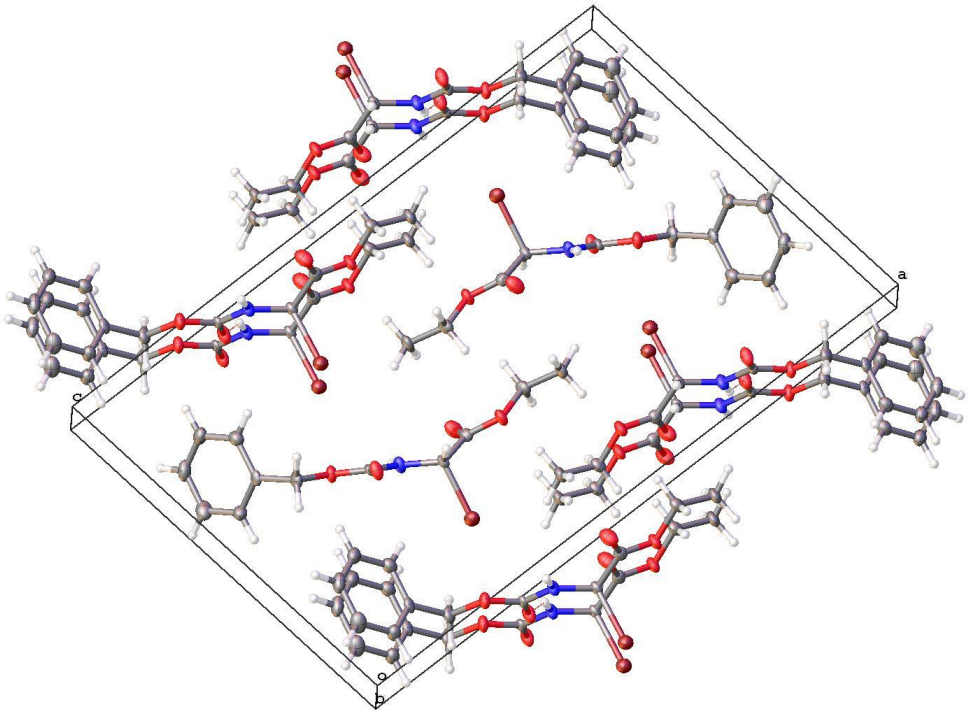

Table SI-7. Crystal data and structure refinement for α-bromoglycine **4c**.

Empirical formula	C12 H14 Br N O4
Formula weight	316.15
Crystal color, shape, size	colorless flat plate, 0.210 × 0.080 × 0.020 mm^3
Temperature	150(2) K
Wavelength	0.71073 Å
Crystal system, space group	Monoclinic, $P2_1/c$
Unit cell dimensions	a = 20.7797(7) Å
	b = 4.8722(2) Å
	c = 13.0682(4) Å
Volume	1305.71(8) $Å^3$
Z	4
Density (calculated)	1.608 Mg/m^3
Absorption coefficient	3.154 mm^{-1}
F(000)	640

Data collection

Diffractometer	APEX II Kappa Duo, Bruker
Theta range for data collection	0.993 to 27.508°.
Index ranges	-27<=h<=26, -6<=k<=6, -16<=l<=16
Reflections collected	18708
Independent reflections	3003 [R_{int} = 0.0385]
Observed Reflections	2527
Completeness to theta = 25.242°	100.0 %

Solution and Refinement

Absorption correction	Semi-empirical from equivalents
Max. and min. transmission	0.7456 and 0.6174
Solution	Intrinsic methods
Refinement method	Full-matrix least-squares on F^2
Weighting scheme	$w = [\sigma^2 Fo^2 + AP^2 + BP]^{-1}$, with
	$P = (Fo^2 + 2\,Fc^2)/3$, A = 0.0282, B = 0.4382
Data / restraints / parameters	3003 / 0 / 168
Goodness-of-fit on F^2	1.040
Final R indices [I>2sigma(I)]	R1 = 0.0246, wR2 = 0.0571
R indices (all data)	R1 = 0.0342, wR2 = 0.0602
Largest diff. peak and hole	0.377 and -0.413 $e.Å^{-3}$

Goodness-of-fit = $[\Sigma[w(F_o^2 - F_c^2)^2]/N_{observns} - N_{params})]^{1/2}$, all data.

R1 = $\Sigma(|F_o| - |F_c|) / \Sigma |F_o|$. $wR2 = [\Sigma[w(F_o^2 - F_c^2)^2] / \Sigma [w(F_o^2)^2]]^{1/2}$.

Table SI-8. Atomic coordinates ($\times 10^4$) and equivalent isotropic displacement parameters ($Å^2 \times 10^3$) for α-bromoglycine **4c**. U(eq) is defined as one third of the trace of the orthogonalized U^{ij} tensor.

Atom	x	y	z	U(eq)
Br1	3054(1)	9082(1)	-2917(1)	30(1)
O1	4511(1)	9192(2)	-1391(1)	21(1)
O2	3982(1)	5710(3)	-767(1)	28(1)
O3	2081(1)	9693(2)	33(1)	21(1)
O4	2497(1)	13298(2)	-726(1)	24(1)
N1	2920(1)	8998(3)	-781(1)	20(1)
C1	5666(1)	9348(4)	-1385(2)	30(1)
C2	5123(1)	7686(4)	-1075(1)	23(1)
C3	3985(1)	7949(4)	-1154(1)	18(1)
C4	3383(1)	9731(4)	-1408(1)	19(1)
C5	2498(1)	10879(3)	-513(1)	17(1)
C6	1596(1)	11517(4)	361(1)	24(1)
C7	1257(1)	9870(4)	1086(1)	20(1)
C8	724(1)	8244(4)	703(1)	27(1)
C9	428(1)	6634(4)	1371(2)	34(1)
C10	667(1)	6648(4)	2421(2)	32(1)
C11	1192(1)	8277(4)	2805(2)	31(1)
C12	1487(1)	9878(4)	2139(1)	25(1)

Table SI-9. Bond lengths [Å] and angles [°] for α-bromoglycine **4c**.

Br1-C4	2.0057(17)	O1-C3	1.329(2)
O1-C2	1.468(2)	O2-C3	1.203(2)
O3-C5	1.3394(19)	O3-C6	1.459(2)
O4-C5	1.211(2)	N1-C5	1.352(2)
N1-C4	1.406(2)	N1-H1N	0.78(2)
C1-C2	1.497(2)	C1-H1A	0.9800
C1-H1B	0.9800	C1-H1C	0.9800
C2-H2A	0.9900	C2-H2B	0.9900
C3-C4	1.516(2)	C4-H4	1.0000
C6-C7	.501(2)	C6-H6A	0.9900
C6-H6B	0.9900	C7-C12	1.382(3)
C7-C8	1.388(3)	C8-C9	1.389(3)
C8-H8	0.9500	C9-C10	1.381(3)
C9-H9	0.9500	C10-C11	1.377(3)
C10-H10	0.9500	C11-C12	1.384(3)
C11-H11	0.9500	C12-H12	0.9500
C3-O1-C2	114.45(13)	C5-O3-C6	115.53(13)

C5-N1-C4	120.73(15)	C5-N1-H1N	119.4(13)
C4-N1-H1N	118.9(13)	C2-C1-H1A	109.5
C2-C1-H1B	109.5	H1A-C1-H1B	109.5
C2-C1-H1C	109.5	H1A-C1-H1C	109.5
H1B-C1-H1C	109.5	O1-C2-C1	108.05(15)
O1-C2-H2A	110.1	C1-C2-H2A	110.1
O1-C2-H2B	110.1	C1-C2-H2B	110.1
H2A-C2-H2B	108.4	O2-C3-O1	124.95(16)
O2-C3-C4	123.36(15)	O1-C3-C4	111.67(14)
N1-C4-C3	110.23(14)	N1-C4-Br1	112.10(12)
C3-C4-Br1	105.24(11)	N1-C4-H4	109.7
C3-C4-H4	109.7	Br1-C4-H4	109.7
O4-C5-O3	124.39(15)	O4-C5-N1	125.28(16)
O3-C5-N1	110.33(15)	O3-C6-C7	106.03(14)
O3-C6-H6A	110.5	C7-C6-H6A	110.5
O3-C6-H6B	110.5	C7-C6-H6B	110.5
H6A-C6-H6B	108.7	C12-C7-C8	119.24(17)
C12-C7-C6	120.33(17)	C8-C7-C6	120.39(16)
C7-C8-C9	120.24(18)	C7-C8-H8	119.9
C9-C8-H8	119.9	C10-C9-C8	119.86(19)
C10-C9-H9	120.1	C8-C9-H9	120.1
C11-C10-C9	120.05(18)	C11-C10-H10	120.0
C9-C10-H10	120.0	C10-C11-C12	120.10(18)
C7-C12-C11	120.51(18)	C7-C12-H12	119.7
C11-C12-H12	119.7		

Table SI-10. Anisotropic displacement parameters ($Å^2 \times 10^3$) for α-bromoglycine **4c**. The anisotropic displacement factor exponent takes the form: $-2\pi^2[h^2 a^{*2} U^{11} + ... + 2 h k a^* b^* U^{12}]$

	U^{11}	U^{22}	U^{33}	U^{23}	U^{13}	U^{12}
Br1	23(1)	43(1)	23(1)	2(1)	2(1)	4(1)
O1	15(1)	20(1)	28(1)	4(1)	3(1)	2(1)
O2	22(1)	17(1)	43(1)	6(1)	2(1)	0(1)
O3	24(1)	16(1)	25(1)	1(1)	11(1)	1(1)
O4	24(1)	14(1)	36(1)	3(1)	10(1)	1(1)
N1	22(1)	12(1)	28(1)	3(1)	10(1)	0(1)
C1	20(1)	39(1)	30(1)	4(1)	5(1)	3(1)
C2	17(1)	22(1)	29(1)	-1(1)	-1(1)	4(1)
C3	17(1)	17(1)	20(1)	-2(1)	1(1)	0(1)
C4	18(1)	16(1)	22(1)	1(1)	4(1)	0(1)
C5	17(1)	17(1)	18(1)	0(1)	1(1)	-2(1)
C6	24(1)	22(1)	28(1)	-1(1)	10(1)	4(1)
C7	19(1)	19(1)	24(1)	-1(1)	7(1)	4(1)
C8	26(1)	33(1)	24(1)	-6(1)	6(1)	-4(1)
C9	30(1)	34(1)	40(1)	-10(1)	13(1)	-11(1)
C10	36(1)	30(1)	35(1)	3(1)	19(1)	1(1)
C11	32(1)	37(1)	24(1)	2(1)	7(1)	8(1)
C12	21(1)	28(1)	27(1)	-4(1)	3(1)	1(1)

Table SI-11. Hydrogen coordinates ($\times 10^4$) and isotropic displacement parameters ($Å^2 \times 10^3$) for α-bromoglycine **4c**

	x	y	z	U(eq)
H1N	2865(9)	7450(40)	-676(14)	13(5)
H1A	6085	8514	-1096	44
H1B	5647	11222	-1120	44
H1C	5621	9394	-2143	44
H2A	5100	5869	-1418	28
H2B	5199	7398	-315	28
H4	3505	11705	-1292	22
H6A	1281	12137	-245	29
H6B	1809	13150	719	29
H8	561	8233	-20	33
H9	63	5526	1107	40
H10	468	5534	2878	39
H11	1352	8300	3528	37
H12	1851	10993	2408	30

Table SI-12. Torsion angles [°] for α-bromoglycine **4c**.

C3-O1-C2-C1	-179.54(14)	C2-O1-C3-O2	-4.1(2)
C2-O1-C3-C4 174.52(13)	174.52(13)	C5-N1-C4-C3	150.45(16)
C5-N1-C4-Br1	-92.68(17)	O2-C3-C4-N1	23.8(2)
O1-C3-C4-N1	-154.83(14)	O2-C3-C4-Br1	-97.27(17)
O1-C3-C4-Br1	84.10(14)	C6-O3-C5-O4	1.0(2)
C6-O3-C5-N1	-179.47(14)	C4-N1-C5-O4	-4.0(3)
C4-N1-C5-O3	176.54(15)	C5-O3-C6-C7	-171.52(14
O3-C6-C7-C12	90.73(19)	O3-C6-C7-C8	-87.0(2)
C12-C7-C8-C9	-0.4(3)	C6-C7-C8-C9	177.34(17)
C7-C8-C9-C10	-0.1(3)	C8-C9-C10-C11	0.7(3)
C9-C10-C11-C12	-0.7(3)	C8-C7-C12-C11	0.3(3)
C6-C7-C12-C11	-177.40(17)	C10-C11-C12-C7	0.2(3)

Table SI-13. Hydrogen bonds for α-bromoglycine **4c** [Å and °].

D-H...A	d(D-H)	d(H...A)	d(D...A)	<(DHA)
N1-H1N...O4#1	0.78(2)	2.16(2)	2.917(2)	164.5(19)
C2-H2B...O2#2	0.99	2.53	3.247(2)	128.9
C4-H4...O2#3	1.00	2.25	3.225(2)	166.1

Symmetry transformations used to generate equivalent atoms:

#1 x,y-1,z #2 -x+1,-y+1,-z #3 x,y+1,z

■ Data supporting the lowest energy conformer through hyperconjugation:

- NMR Spectroscopy. Vicinal J_{NH-CH} coupling constant in ^1H NMR ~ 10 Hz
- X-ray analysis. d(C-Br) = 2.006 Å; torsion angle α(C-N-$^{\alpha}$C-Br)= -92.5 °
- Weak Hydrogen bond NH···OCOEt ~ 2.4 Å confirmed by X-ray (2.491 Å) and N-H···O bond angle of 99.1 °

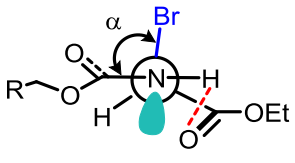

dihedral angle C-N-$^{\alpha}$C-C
Φ = 150.5 °

A *(sc; g+)*
lone pair aligns antiperiplanar to σ^*_{C-X} *& ester-carbamate away*

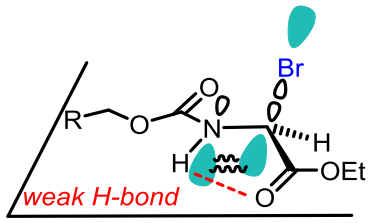

hyperconjugation:
Filled $N_{(sp2)}$ interacts with $\sigma^*_{(C-Br)}$

The dihedral angles observed in the crystal packing of the X-ray correlates with the conformational analysis calculations. The Φ torsion angle between the C-N-$^{\alpha}$C and N-$^{\alpha}$C-C(O_2Et) planes (Φ = 150.5 ^{o}) and the θ torsion angle between the H-N-$^{\alpha}$C and N-$^{\alpha}$C-H planes (θ = -161.9 ^{o}) supports the observed vicinal coupling constant by ^{1}H NMR J_{NH-CH}= 10 Hz. Furthermore the quasi-orthogonality of the dihedral angle α between C-N-$^{\alpha}$C-Br (α = -92.5 ^{o}) likely supports the fact that the nitrogen lone pair not only engage in conjugation with the carbonyl π* orbital (Cbz-carbamate), but is also closely aligned (antiperiplanar) with the σ^*_{C-Br} orbital to achieve a spatial electronic donation through hyperconjugation. This unique phenomenon of hyperconjugation is also supported by the abnormal bond length observed in the α-bromoglycine **4c** crystal structure with a $^{\alpha}$carbon-bromine distance of 201 pm which is 4 pm larger than the mean C_{sp3}–Br bond length of 197 pm reported in the literature.[SI-4]

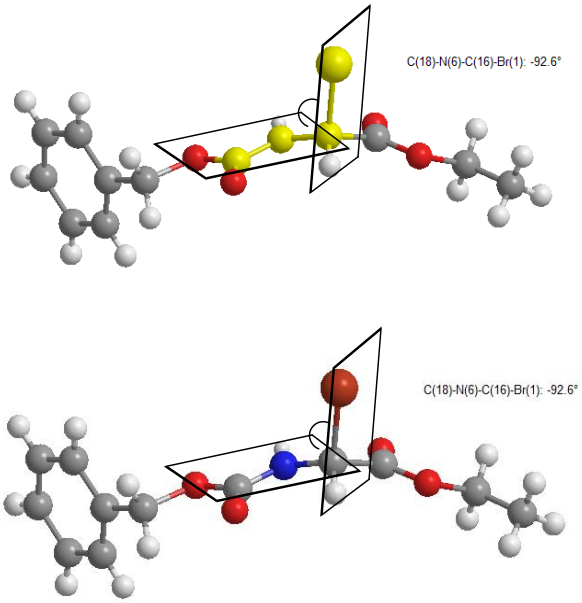

[SI-4] Allen, F. H.; Kennard, O.; Watson, D. G.; Brammer, L.; Orpen, A. G.; Taylor, R. *J. Chem. Soc., Perkin Transactions 2* **1987**, S1-S19.

b) Density Functional Theory (DFT) Analysis of α-Haloglycine Esters

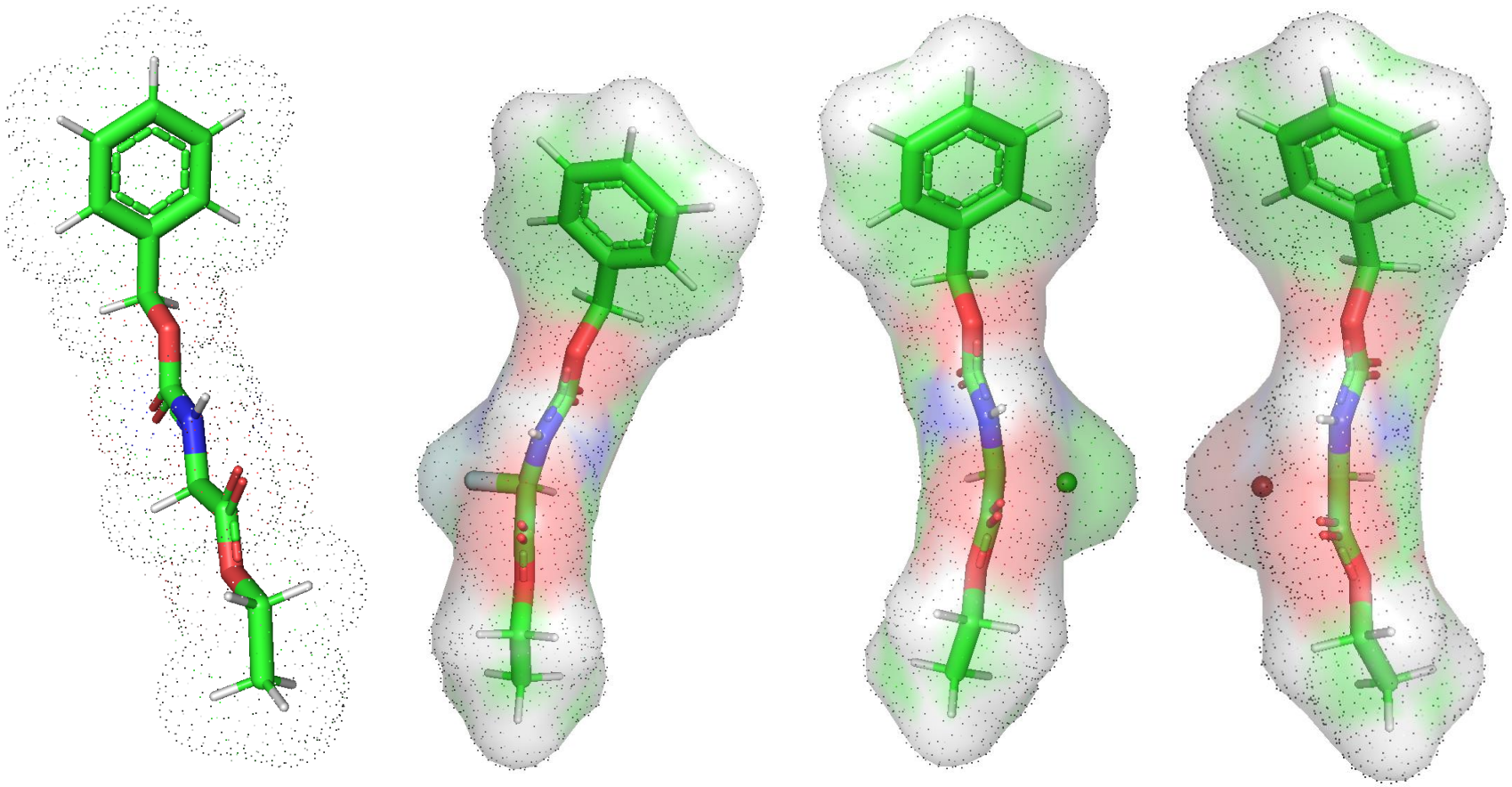

Figure SI-18: From left to right: glycine A= H, α-fluorolycine **4a**: A= F, α-chlorolycine **4b**: A= Cl α-bromolycine **4c**: A= Br

Similarly to the well-established reactivity of (C1-halogenated) glycosyl halides during glycosidic bond formation, it appears that α-haloglycine esters (X = F, Cl or Br) are prone to heterolysis (self-ionization) at low temperature (-78 °C). This phenomenon likely indicates that a dynamic equilibrium is taking place between the covalently bond halogen C20-X (see below C20-A values on page S43) and a contact ion pair (CIP) which is a similar scenario proposed to explain the reactivity of glycosyl halides via anomeric effect. As we are studying the effect of thioureas as H-bond donor, and anion binder catalysts, we became interested in characterizing the innate tendency of α-haloglycines to ionize to the corresponding CIP-carbocation to assess the possibility of a "generalized" anomeric effect on these acyclic molecules. Therefore *in silico* studies have been undertaken and will be supported by spectroscopic characterizations to confirm the impact of the proposed anomeric effect, result of hyperconjugation (IR, NMR and X-ray).

Computational Methods: Calculations were performed using the Gaussian 09 program (Revisions A.02).[SI-5] The geometries of several ground-state conformers were fully optimized (4 conformers assessed for each molecule: *syn, gauche, gauche ' and anti*) at the B3LYP 6-311++G (3df,3pd) level of theory with the conductor like polarizable continuum model of solvation, CPCM(DCM).[SI-6] In each case, the results of geometry optimization on **4a**,**4b** and **4c** suggested that a *gauche* conformation corresponded to the lowest energy conformers as shown by the calculated ΔG^{o} of stabilization for the *gauche* conformers (Table page S35). The computed *gauche* conformers presented always a C20–A32 bond considerably elongated and a C20–N18 bond shortened which is accord with previous reports of anomeric effects (see references [35] and specifically [35e]). Only the minimized gauche conformers are reported in the SI (see Figure SI-18). Reported electronic energies do not include zero point energy (ZPE) corrections. To determine free energies, the thermal corrections evaluated from the unscaled vibrational frequencies at the initial level of optimization were added to the single-point electronic energies. All molecular structures were rendered in Pymol. The optimized structure of α-haloglycine esters (*gauche*-

---

[SI-5] M. J. Frisch, G. W. Trucks, H. B. Schlegel, G. E. Scuseria, M. A. Robb, J. R. Cheeseman, G. Scalmani, V. Barone, B. Mennucci, G. A. Petersson, H. Nakatsuji, M. Caricato, X. Li, H. P. Hratchian, A. F. Izmaylov, J. Bloino, G. Zheng, J. L. Sonnenberg, M. Hada, M. Ehara, K. Toyota, R. Fukuda, J. Hasegawa, M. Ishida, T. Nakajima, Y. Honda, O. Kitao, H. Nakai, T. Vreven, J. A. Montgomery, Jr., J. E. Peralta, F. Ogliaro, M. Bearpark, J. J. Heyd, E. Brothers, K. N. Kudin, V. N. Staroverov, R. Kobayashi, J. Normand, K. Raghavachari, A. Rendell, J. C. Burant, S. S. Iyengar, J. Tomasi, M. Cossi, N. Rega, J. M. Millam, M. Klene, J. E. Knox, J. B. Cross, V. Bakken, C. Adamo, J. Jaramillo, R. Gomperts, R. E. Stratmann, O. Yazyev, A. J. Austin, R. Cammi, C. Pomelli, J. W. Ochterski, R. L. Martin, K. Morokuma, V. G. Zakrzewski, G. A. Voth, P. Salvador, J. J. Dannenberg, S. Dapprich, A. D. Daniels, O. Farkas, J. B. Foresman, J. V. Ortiz, J. Cioslowski, and D. J. Fox, Gaussian, Inc., Wallingford CT, **2009**.

[SI-6] Scalmani, G.; Frisch, M. J. *J. Chem. Phys.* **2010**, *132*, 114110.

conformers) were used to calculate the NMR spectra at B3LYP method with 6-311++G(2d,p) level using the GIAO method, and the chemical shifts of the compound are reported in ppm relative to TMS for ^{1}H NMR spectra which are presented below.

We further evaluated the % of ionic-character in the different α-haloglycine esters **4a-c** which would be a good indicator of electrofugacity of the different halogens (X = F, Cl or Br) and possibly relate these results to an hyperconjugation effect $n_{(\alpha N)}$ donation to $\sigma^*_{(C\text{-}X)}$ typically characteristic of an anomeric effect. To this purpose, glycine (A =H) as well as the glycinyl carbocation have been also evaluated at the B3LYP 6-311++G (3df,3pd) level of theory. The glycine molecule has been selected for the model of 0% ionization character and the carbocation.

Level of theory: DFT B3LYP 6-311++G (3df,3pd); CPCM solvent: DCM

Electronegativity		**Bond C3-A (Å)**		**Typical bond length (Å)**	**Calculated glycine (Å)**
H: 2.2	Lit (Avg C_{sp3}-X)		Lit (Avg anomeric effect)		
F: 4.1	C-F	1.349	1.395 (Δd = +5 pm)	C2(sp^2)-C3(sp^3) ~1.500	1.526
Cl: 2.8	C-Cl	1.790	1.808 (Δd = +2 pm)	C3(sp^3)-N4(sp^2) ~1.454	1.439
Br: 2.7	C-Br	1.966	1.991 (Δd = +2 pm)	C3(sp^3)-H7 ~1.099	1.088

Hartrees	**H**	**F**	**Cl**	**Br**	**OH**	**carbocation**
($E_{electronic}$)	-822.31	-921.58	1281.93	3395.85	-897.56	-821.47
ZPE	0.26	0.25	0.25	0.25	0.26	0.25
$U_{298K\ corr.}$	0.28	0.27	0.27	0.27	0.28	0.27
$H_{298K\ corr.}$	0.28	0.27	0.27	0.27	0.28	0.27
$G_{298K\ corr.}$	0.21	0.20	0.20	0.20	0.21	0.20
($E_{electronic}$) + ZPE	-822.05	-921.33	1281.68	3395.60	-897.29	-821.22
($E_{electronic}$) + $U_{298K\ corr.}$	-822.03	-921.31	1281.66	3395.59	-897.27	-821.20
($E_{electronic}$) + $H_{298K\ corr.}$	-822.03	-921.31	1281.66	3395.58	-897.27	-821.20
($E_{electronic}$) + $G_{298K\ corr.}$	-822.10	-921.38	1281.73	3395.66	-897.34	-821.27
ΔG^o (kcal/mol) Stabilization of the gauche rotamer	**-0.33**	**-0.74**	**-0.44**	**-1.07**	**-1.02**	**-1.93**

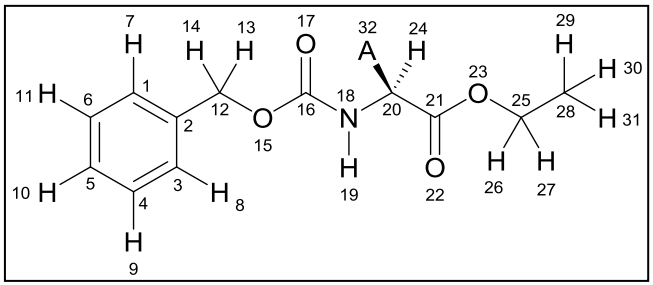

Level of theory:
DFT B3LYP 6-311++G (3df,3pd)

Glycine: A = H, **SI-1**

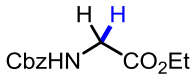


```
Symbolic Z-matrix:
 Charge =  0 Multiplicity = 1
 C                     4.41234  -0.65253   1.15988
 C                     4.10503  -0.38218  -0.18042
 C                     5.0784    0.16802  -1.02526
 C                     6.35908   0.44786  -0.52981
 C                     6.66639   0.1775    0.81049
 C                     5.69302  -0.3727    1.65533
 H                     3.66915  -1.07262   1.80493
 H                     4.84376   0.37445  -2.0486
 H                     7.10227   0.86795  -1.17486
 H                     7.64422   0.39116   1.18877
 H                     5.92766  -0.57912   2.67867
 C                     2.69769  -0.68969  -0.72487
 H                     2.76244  -0.92947  -1.76565
 H                     2.28297  -1.52015  -0.19266
 O                     1.85859   0.45508  -0.55076
 C                     0.55178   0.16953  -1.05632
 O                     0.40876  -0.63992  -2.00917
 N                    -0.51866   0.76286  -0.51636
 H                    -0.40501   1.4061    0.24082
 C                    -1.86203   0.46933  -1.03607
 C                    -2.76567   1.70216  -0.84856
 O                    -2.56538   2.48867   0.11313
 O                    -3.83238   1.95316  -1.76728
 H                    -1.79728   0.22955  -2.07685
 C                    -4.05923   3.36194  -1.86093
 H                    -4.32087   3.74592  -0.89708
 H                    -3.16917   3.84428  -2.20742
 C                    -5.20798   3.63226  -2.85032
 H                    -6.09804   3.14993  -2.50383
 H                    -5.37773   4.68638  -2.92039
 H                    -4.94634   3.24828  -3.81417
 H                    -2.27675  -0.36113  -0.50387
```

Computed total energy:

E(RB3LYP) = -822.30875496 a.u.

α-Fluoroglycine: A = F, **4a**

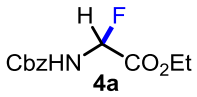


```
Symbolic Z-matrix:
 Charge =  0 Multiplicity = 1
 C                     4.41234  -0.65253   1.15988
 C                     4.10503  -0.38218  -0.18042
 C                     5.0784    0.16802  -1.02526
 C                     6.35908   0.44786  -0.52981
 C                     6.66639   0.1775    0.81049
 C                     5.69302  -0.3727    1.65533
 H                     3.66915  -1.07262   1.80493
 H                     4.84376   0.37445  -2.0486
 H                     7.10227   0.86795  -1.17486
 H                     7.64422   0.39116   1.18877
 H                     5.92766  -0.57912   2.67867
 C                     2.69769  -0.68969  -0.72487
 H                     2.76244  -0.92947  -1.76565
 H                     2.28297  -1.52015  -0.19266
 O                     1.85859   0.45508  -0.55076
 C                     0.55178   0.16953  -1.05632
 O                     0.40876  -0.63992  -2.00917
 N                    -0.51866   0.76286  -0.51636
 H                    -0.40501   1.4061    0.24082
 C                    -1.86203   0.46933  -1.03607
 C                    -2.76567   1.70216  -0.84856
 O                    -2.56538   2.48867   0.11313
 O                    -3.83238   1.95316  -1.76728
 H                    -1.79728   0.22955  -2.07685
 C                    -4.05923   3.36194  -1.86093
 H                    -4.32087   3.74592  -0.89708
 H                    -3.16917   3.84428  -2.20742
 C                    -5.20798   3.63226  -2.85032
 H                    -6.09804   3.14993  -2.50383
 H                    -5.37773   4.68638  -2.92039
 H                    -4.94634   3.24828  -3.81417
 F                    -2.38527  -0.57845  -0.3646
```

Computed total energy:

E(RB3LYP) = -921.58266843 a.u.

α-Chloroglycine: A = Cl, **4b**

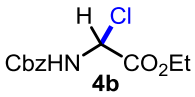

4b

```
Symbolic Z-matrix:
 Charge =  0 Multiplicity = 1
 C                     4.41234  -0.65253   1.15988
 C                     4.10503  -0.38218  -0.18042
 C                     5.0784    0.16802  -1.02526
 C                     6.35908   0.44786  -0.52981
 C                     6.66639   0.1775    0.81049
 C                     5.69302  -0.3727    1.65533
 H                     3.66915  -1.07262   1.80493
 H                     4.84376   0.37445  -2.0486
 H                     7.10227   0.86795  -1.17486
 H                     7.64422   0.39116   1.18877
 H                     5.92766  -0.57912   2.67867
 C                     2.69769  -0.68969  -0.72487
 H                     2.76244  -0.92947  -1.76565
 H                     2.28297  -1.52015  -0.19266
 O                     1.85859   0.45508  -0.55076
 C                     0.55178   0.16953  -1.05632
 O                     0.40876  -0.63992  -2.00917
 N                    -0.51866   0.76286  -0.51636
 H                    -0.40501   1.4061    0.24082
 C                    -1.86203   0.46933  -1.03607
 C                    -2.76567   1.70216  -0.84856
 O                    -2.56538   2.48867   0.11313
 O                    -3.83238   1.95316  -1.76728
 H                    -1.79728   0.22955  -2.07685
 C                    -4.05923   3.36194  -1.86093
 H                    -4.32087   3.74592  -0.89708
 H                    -3.16917   3.84428  -2.20742
 C                    -5.20798   3.63226  -2.85032
 H                    -6.09804   3.14993  -2.50383
 H                    -5.37773   4.68638  -2.92039
 H                    -4.94634   3.24828  -3.81417
 Cl                   -2.54418  -0.89666  -0.16067
```

Computed total energy:

E(RB3LYP) = -1281.93467664 a.u.

α-Bromoglycine: A = Br, **4c**

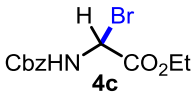


```
Symbolic Z-matrix:
 Charge =  0 Multiplicity = 1
 C                     4.41234  -0.65253   1.15988
 C                     4.10503  -0.38218  -0.18042
 C                     5.0784    0.16802  -1.02526
 C                     6.35908   0.44786  -0.52981
 C                     6.66639   0.1775    0.81049
 C                     5.69302  -0.3727    1.65533
 H                     3.66915  -1.07262   1.80493
 H                     4.84376   0.37445  -2.0486
 H                     7.10227   0.86795  -1.17486
 H                     7.64422   0.39116   1.18877
 H                     5.92766  -0.57912   2.67867
 C                     2.69769  -0.68969  -0.72487
 H                     2.76244  -0.92947  -1.76565
 H                     2.28297  -1.52015  -0.19266
 O                     1.85859   0.45508  -0.55076
 C                     0.55178   0.16953  -1.05632
 O                     0.40876  -0.63992  -2.00917
 N                    -0.51866   0.76286  -0.51636
 H                    -0.40501   1.4061    0.24082
 C                    -1.86203   0.46933  -1.03607
 C                    -2.76567   1.70216  -0.84856
 O                    -2.56538   2.48867   0.11313
 O                    -3.83238   1.95316  -1.76728
 H                    -1.79728   0.22955  -2.07685
 Br                   -2.60232  -1.01308  -0.08606
 C                    -4.05923   3.36194  -1.86093
 H                    -4.32087   3.74592  -0.89708
 H                    -3.16917   3.84428  -2.20742
 C                    -5.20798   3.63226  -2.85032
 H                    -6.09804   3.14993  -2.50383
 H                    -5.37773   4.68638  -2.92039
 H                    -4.94634   3.24828  -3.81417
```

Computed total energy:

E(RB3LYP) = -3395.85557774 a.u.

α-Acetoxyglycine : A = OAc

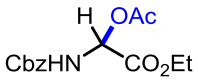


```
Symbolic Z-matrix:
 Charge =  0 Multiplicity = 1
 C                     3.91071  -1.07184   0.74757
 C                     3.72761  -0.48616  -0.51234
 C                     4.74378   0.29793  -1.07493
 C                     5.94307   0.49635  -0.3776
 C                     6.12618  -0.08933   0.88231
 C                     5.11     -0.87342   1.44489
 H                     3.13484  -1.67051   1.17711
 H                     4.60398   0.74511  -2.0369
 H                     6.71894   1.09503  -0.80714
 H                     7.04186   0.06217   1.41474
 H                     5.2498   -1.3206    2.40686
 C                     2.40971  -0.7042   -1.27864
 H                     2.59959  -0.67193  -2.33116
 H                     1.9999   -1.65797  -1.01923
 O                     1.47988   0.32484  -0.93024
 C                     0.25612   0.12238  -1.6418
 O                     0.27003  -0.42683  -2.77395
 N                    -0.90344   0.51679  -1.10394
 H                    -0.9145    0.95321  -0.20427
 C                    -2.16144   0.30865  -1.8354
 C                    -3.16279   1.41685  -1.46021
 O                    -3.11923   1.94399  -0.31837
 O                    -4.14213   1.84688  -2.40935
 H                    -1.97156   0.34093  -2.88793
 C                    -4.45475   3.22352  -2.18124
 H                    -4.84186   3.34198  -1.19078
 H                    -3.56876   3.81336  -2.29082
 C                    -5.50942   3.68662  -3.2034
 H                    -6.39541   3.09677  -3.09383
 H                    -5.74333   4.71669  -3.03272
 H                    -5.1223    3.56815  -4.19386
 O                    -2.70913  -0.966    -1.48871
 C                    -2.96288  -1.00914  -0.08207
 O                    -2.06948  -1.41387   0.70634
 C                    -4.32949  -0.56029   0.46795
 H                    -4.99252  -1.39933   0.5039
 H                    -4.20415  -0.16227   1.45322
 H                    -4.74134   0.19261  -0.17114
```

Computed total energy:

E(RB3LYP) = -1050.27310878 a.u.

α-Hydroxyglycine: A = OH, **3**

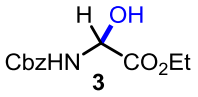

Symbolic Z-matrix:
Charge = 0 Multiplicity = 1

C	4.41234	-0.65253	1.15988
C	4.10503	-0.38218	-0.18042
C	5.0784	0.16802	-1.02526
C	6.35908	0.44786	-0.52981
C	6.66639	0.1775	0.81049
C	5.69302	-0.3727	1.65533
H	3.66915	-1.07262	1.80493
H	4.84376	0.37445	-2.0486
H	7.10227	0.86795	-1.17486
H	7.64422	0.39116	1.18877
H	5.92766	-0.57912	2.67867
C	2.69769	-0.68969	-0.72487
H	2.76244	-0.92947	-1.76565
H	2.28297	-1.52015	-0.19266
O	1.85859	0.45508	-0.55076
C	0.55178	0.16953	-1.05632
O	0.40876	-0.63992	-2.00917
N	-0.51866	0.76286	-0.51636
H	-0.40501	1.4061	0.24082
C	-1.86203	0.46933	-1.03607
C	-2.76567	1.70216	-0.84856
O	-2.56538	2.48867	0.11313
O	-3.83238	1.95316	-1.76728
H	-1.79728	0.22955	-2.07685
C	-4.05923	3.36194	-1.86093
H	-4.32087	3.74592	-0.89708
H	-3.16917	3.84428	-2.20742
C	-5.20798	3.63226	-2.85032
H	-6.09804	3.14993	-2.50383
H	-5.37773	4.68638	-2.92039
H	-4.94634	3.24828	-3.81417
O	-2.41628	-0.64054	-0.32481
H	-3.01174	-1.12533	-0.90101

Computed total energy:

E(RB3LYP) = -897.55757755 a.u.

Glycinyl Iminium SI-II

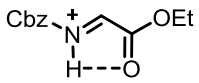

SI-II

Symbolic Z-matrix:
Charge = 1 Multiplicity = 1

C	-4.34612	0.51242	0.88456
C	-3.66083	0.25062	-0.302
C	-4.10538	-0.78254	-1.12723
C	-5.2119	-1.5451	-0.77121
C	-5.88675	-1.27906	0.41608
C	-5.45307	-0.24818	1.2437
H	-4.01377	1.31713	1.52791
H	-3.58515	-0.98775	-2.05414
H	-5.54917	-2.34154	-1.4206
H	-6.74994	-1.86929	0.69272
H	-5.97801	-0.03432	2.16483
C	-2.45836	1.06199	-0.68174
H	-2.33635	1.11792	-1.76131
H	-2.51035	2.07184	-0.28045
O	-1.28095	0.40975	-0.12293
C	-0.10588	1.00536	-0.36722
O	0.04445	2.02356	-1.0061
N	0.91255	0.28631	0.20522
H	0.69557	-0.54625	0.73261
C	2.24715	0.6989	0.13416
C	3.18768	-0.50543	0.27171
O	2.83848	-1.56783	0.72431
O	4.40347	-0.19769	-0.14199
H	2.43408	1.27052	-0.76916
C	5.43291	-1.22405	-0.01576
H	5.50965	-1.49302	1.03618
H	5.10489	-2.09774	-0.57577
C	6.72058	-0.65009	-0.55443
H	7.02437	0.22993	0.01087
H	7.50737	-1.39942	-0.47026
H	6.6194	-0.377	-1.60401

Computed total energy:

E(RB3LYP) = -821.47193795 a.u.

	Bond length (Å)										
A	C21-O23	C21-C20	C20-N18	N18-C16	C16-O15	C21=O	C20-A32	C20-H24	N18-H19	C16=O	O22-H19
SI-I: H	1.328	1.514	1.441	1.349	1.352	1.209	1.092	1.092	1.008	1.219	2.277
OH	1.326	1.537	1.418	1.362	1.346	1.207	1.430	1.089	1.008	1.214	2.355
OAc	1.324	1.540	1.414	1.365	1.343	1.205	1.449	1.087	1.007	1.214	2.564
4a: F	1.321	1.534	1.399	1.372	1.340	1.206	1.420	1.085	1.009	1.211	2.374
4b: Cl	1.321	1.525	1.394	1.374	1.338	1.206	1.881	1.081	1.010	1.211	2.392
4c: Br	1.321	1.519	1.386	1.377	1.337	1.207	2.082	1.080	1.010	1.210	2.394
SI-II: Cation	1.307	1.513	1.272	1.478	1.298	1.203	NA	1.024	1.083	1.190	2.351

% ionic character were calculated as follows: = 1-[(bond length molecule of interest – bond length in **SI-II**)/(bond length in **SI-I** – bond length in **SI-II**)] In this formula we considered clycine **SI-I** to be 0% ionized and the carbocation (iminium) **SI-II** to be the 100% ionized. [a] For the C20-A32 bond, the formula cannot be applied given that no bond length can be obtained for the carbocation **SI-II**. Given that A32 is the leaving atom from the molecules, the ionization character was calculated as follows: % ionic character = 1-[(C20-A32 bond length molecule of interest – sum of the VdW radius) / (bond length literature – sum of the VdW radius)] in which the sum of VdW represents the 100% ionization.

	Proposed % Ionic character based on Bond length Elongation										
SI-1: H	0%	0%	0%	0%	0%	0%	0%	0%	0%	0%	NA
OH	10%	23%	13%	10%	11%	10%	1%	4%	0%	15%	NA
OAc	20%	26%	16%	13%	16%	24%	1%	7%	-1%	17%	NA
4a: F	36%	20%	25%	18%	22%	14%	4%	10%	2%	25%	NA
4b: Cl	36%	35%	28%	19%	25%	14%	5.5%	16%	2%	27%	NA
4c: Br	32%	47%	33%	21%	28%	10%	7%	18%	3%	30%	NA
SI-II: Cation	100%	100%	100%	100%	100%	100%	NA	100%	100%	100%	NA

Van der Walls radius: C = 170; O = 152; F = 147; Cl = 175; Br = 185

IR Calculations:

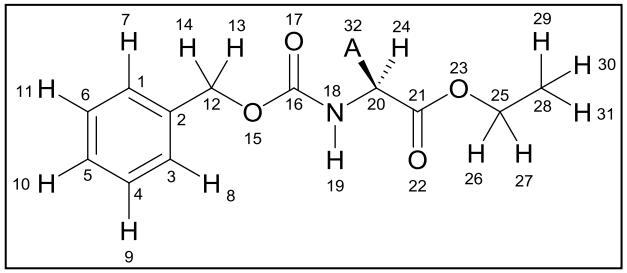

Calculated Frequency : IR (cm^{-1})				Experimental FT-IR (cm^{-1})
A	C21=O22	C16=O17	N18–H19	C21=O22
H	1758.97	1719.71	3610.14	1728
OH	1768.64	1734.52	3609.89	ND
OAc	1773.83	1739.16	3621.1	ND
4a: F	1773.38	1745.04	3599.5	ND
4b: Cl	1768.48	1745.5	3593.77	1742
4c: Br	1764.34	1747.64	3585.78	1736

Conclusion from IR calculation: The IR frequency of the C=O group of the ester moiety for **4b** and **4c** shows similar pattern (Δ = ~ 4 cm^{-1}) between calculated and experimental value. Which suggest the **4b** and **4c** are also stabilized by a weak internal hydrogen bond NH···O=C (2.491 Å) and the carbonyl π^* orbital of the ester is in alignment with the C–Cl and C–Br bond.

NMR Chemical Shifts by GIAO Calculations:

^{1}H NMR δ (ppm)	H7	H8	H9	H10	H11	H13	H14	H19	H24	H26	H27	H29-31
SI-I: H	8.00	8.00	8.00	7.93	8.00	5.22	5.22	5.70	4.32	4.45	4.45	1.59
F	8.07	8.04	7.98	7.93	8.03	5.36	5.35	6.81	6.60	4.49	4.58	1.70
Cl	8.05	7.99	8.07	8.16	8.08	5.26	5.37	6.43	6.77	4.46	4.56	1.67
Br	8.06	8.03	8.03	7.96	8.01	5.30	5.44	6.59	7.02	4.46	4.57	1.67
OH	8.06	8.04	7.97	7.90	8.01	5.32	5.30	6.48	6.08	4.41	4.54	1.67
OAc	8.02	8.02	7.99	8.01	8.03	5.27	5.32	6.51	6.26	4.32	4.49	1.57
SI-II	8.13	8.13	11.33	8.12	8.12	8.12	5.93	5.98	9.34	4.93	4.95	1.85

α-haloglycine	Theoretical Value in CH_2Cl_2	^{1}H NMR in $CDCl_3$ Experimental	^{1}H NMR in CD_3CN Experimental	Δδ(ppm) $CDCl_3$ vsCD_3CN	J constant and torsional angle Φ(HNC$^{\alpha}$H)
4a: F	6.60 ppm	6.09 ppm (dd, *J* = 9.0, 53.8 Hz).	5.95 ppm (dd, *J* = 9.5, 53.7 Hz)	0.14	Φ ~-120^{O} or +60 ^{o}
4b: Cl	6.77 ppm	6.17 ppm (d, *J* = 10.3 Hz).	6.18 ppm (d, *J* = 10.4 Hz)	- 0.01	Φ ~-120 ^{O}
4c: Br	7.02 ppm	6.36 ppm (d, *J* = 10.2 Hz).	6.39 ppm(d, *J* = 10.8 Hz)	- 0.03	Φ ~-120 ^{O}

Conclusion of the preliminary calculations: The $J_{NH\text{-}CH}{}^{\alpha}$ coupling constants for **4a**, **4b** and **4c** are abnormally large in both $CDCl_3$ or CD_3CN (> 9.0 Hz), suggesting that α-haloglycines **4a-c** have similar conformations in solution as shown below.

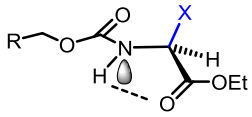

Prefered conformation

The DFT results suggests that the reactivity order of the haloglycine is following Br > Cl > F trends, as the ease of ion pair formation is related to the ionic character of the C–X bond. This unique phenomenon of hyperconjugation in the α-bromoglycine **4c** is further characterized by the abnormal (C20)–N and C(20)–Br bond lengths as seen in the X-ray crystal structure. The C(20)–Br length of 201 pm is the longest ever reported C–Br bond, +4 pm longer than the average Csp^3–Br bond lengths reported in the literature.

Hyperconjugation, bond length and hybridization correlations.

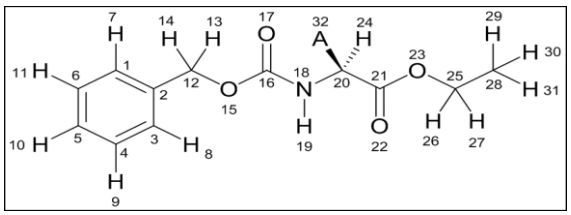

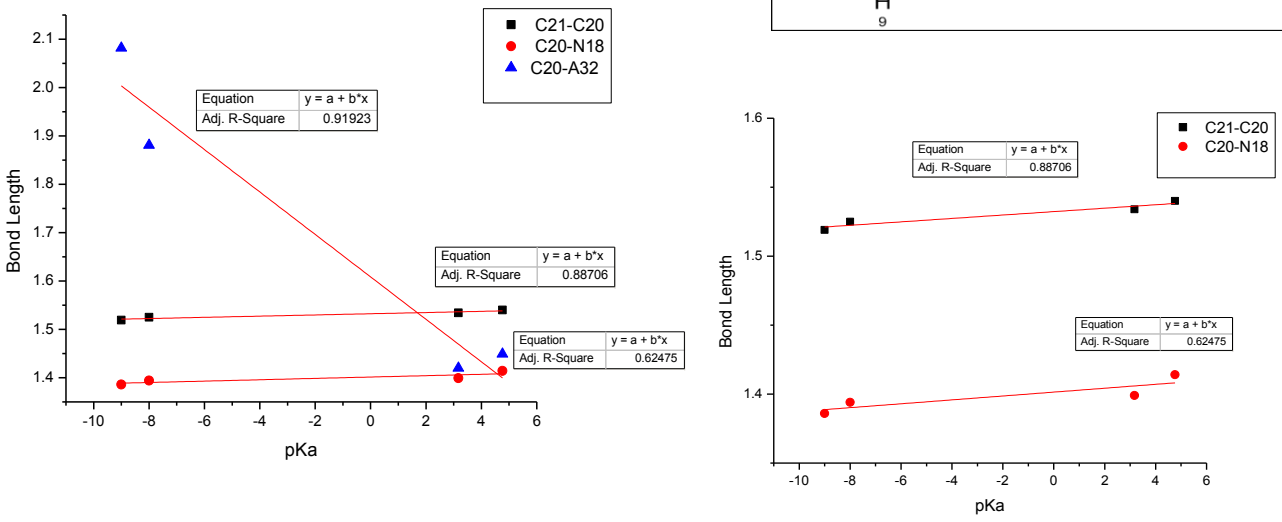

Figure SI-19: Bond length and pKa correlation: Acetate (AcOH, pKa = 4.8; HF, pKa = 3.2; HCl, pKa = -8.0; HBr pKa = -9.0)

Given that upon anomeric affect, the changes in bond length are apparent well before significant changes in torsion angles arise, bond length elongation could be correlated to the leaving group ability and its propensity to hyperconjugation. Bond lengths (C20–A32, C20–N18, C2–C21) have been correlated with the pKas (in H_2O) of the leaving groups' conjugated acids (Figure SI-19). It appears that a linear relationship between the two values can be established with a trend for the bond elongating/breaking C20–A32 and the two bonds shortening C20–N18 and C20–C21 which suggest an increasing sp^2 character depending on the leaving group from acetate and fluoride to chloride and finally bromide exerting the stronger effect.

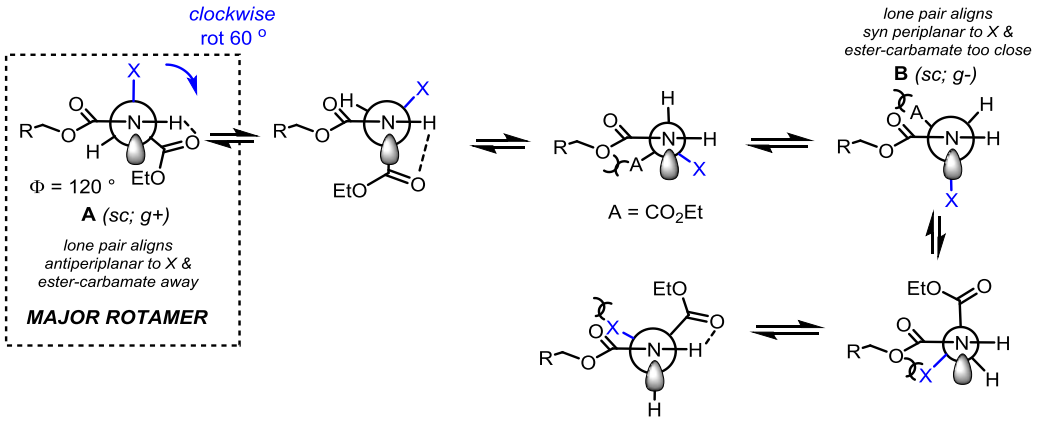

V. Supplemental Procedure and Compounds Characterization:

Procedure for halogen-exchange from α-fluoroglycine esters 4a:

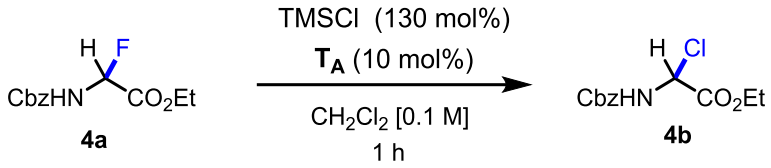

In a flame dried scintillation vial, α-fluoroglycine **4a** (64 mg, 0.25 mmol, 1.0 eq.) was dissolved in anhydrous dichloromethane (2.5 mL [0.1 M]). The reaction mixture was then cool down to -78 °C and the thiourea catalyst $\mathbf{T_A}$ (10 mol%) was added in one portion. TMSCl (1.3 eq.) was then added dropwise to the reaction mixture which was stirred for 1 hour. To monitor the reaction, aliquots were taken and evaporated, at the desired reaction times, using the rotary evaporator (caution: bath at 0°C) and short period on high vacuum to obtain the data points of reaction advancement.

Recording data points to assess the reaction course: Into the crude reaction mixture vial, the internal standard mesitylene (30 mg, 0.25 mmol) was accurately weighted and dissolved in the NMR solvent CD_3CN (2.5 mL). Approximately 400 µL of the sample was taken into an NMR tube and the ^1H NMR spectrum were recorded within short period of time to avoid sample hydrolysis and decomposition.

Selected Spectra:

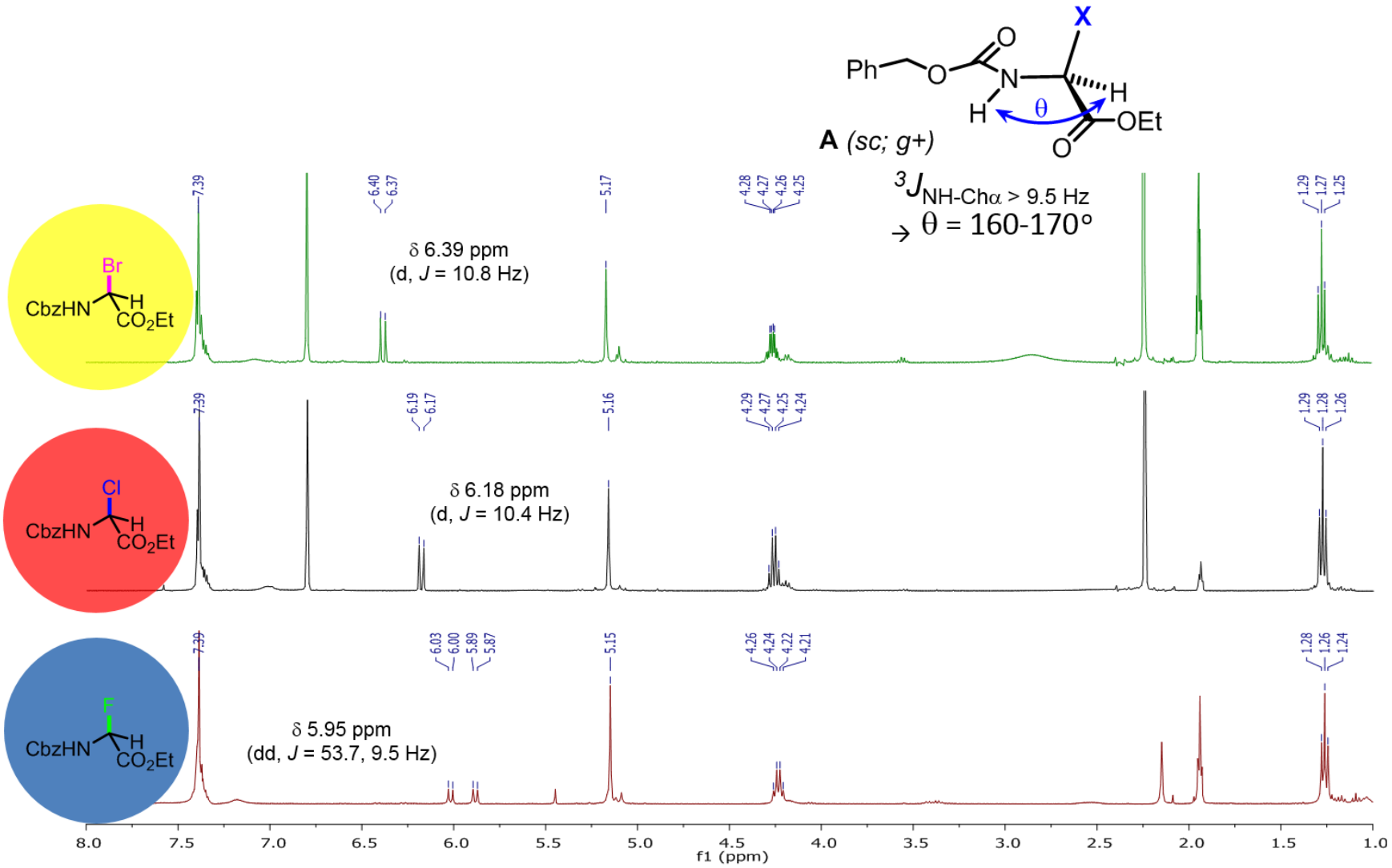

Figure SI-20. ^{1}H NMR Overlay of Fluoroglycine **4a**, Chloroglycine **4b** and Bromoglycine **4c** in CD_3CN

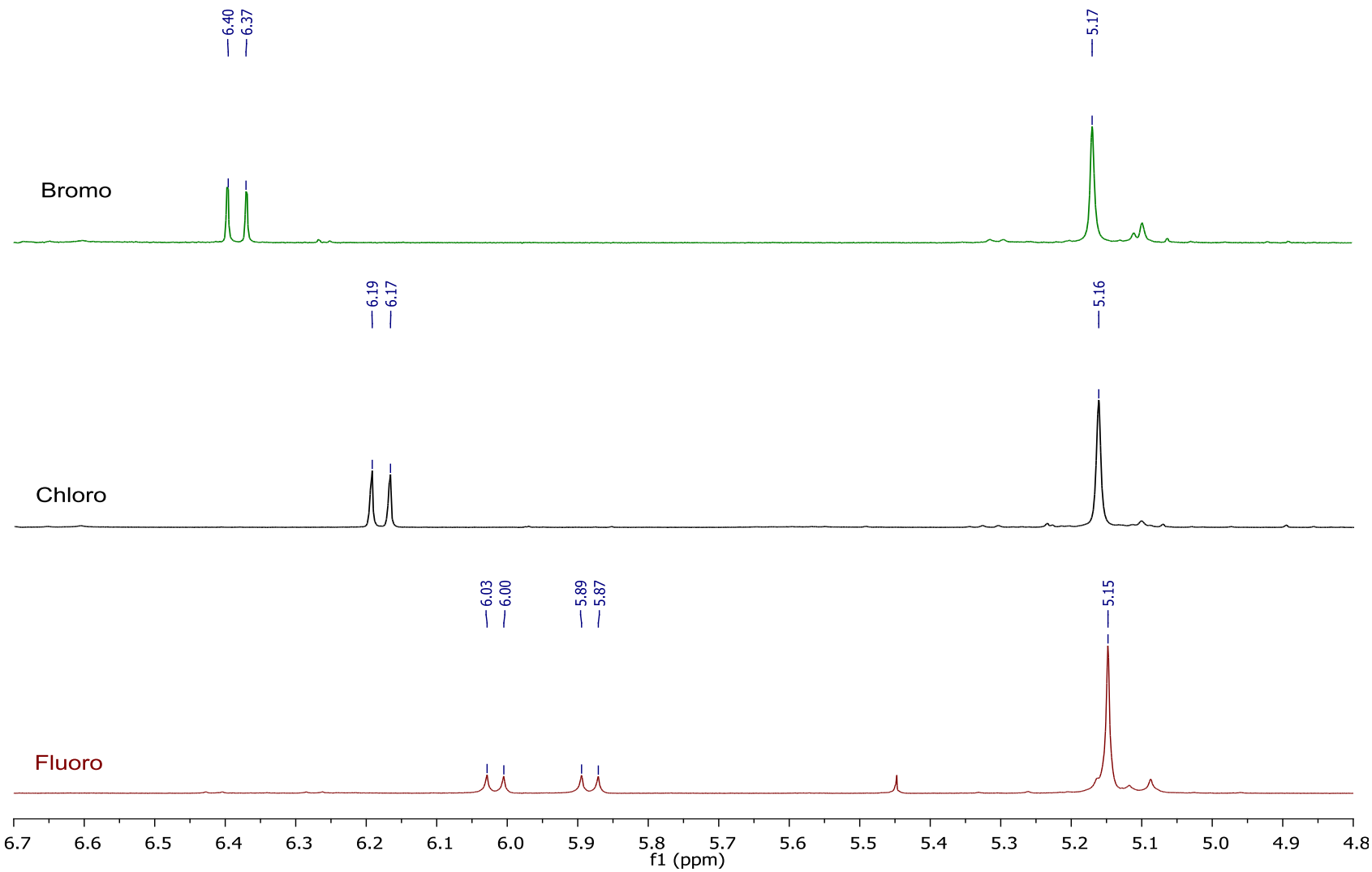

Figure SI-21. ^{1}H NMR Overlay of Fluoroglycine **4a**, Chloroglycine **4b** and Bromoglycine **4c** in **CD_3CN**

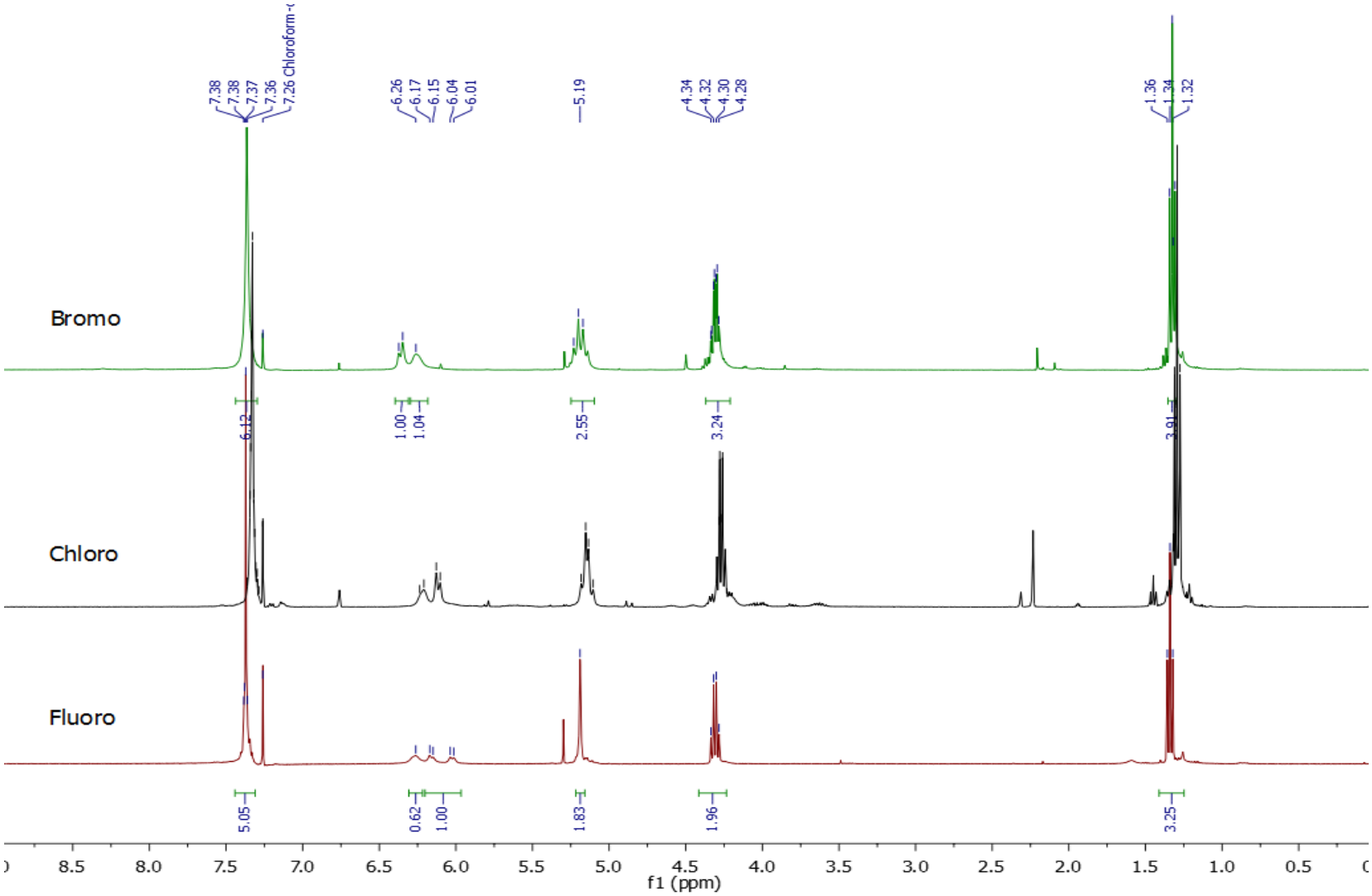

Figure SI-22.[1]H NMR Overlay of Fluoroglycine **4a**, Chloroglycine **4b** and Bromoglycine **4c** in **$CDCl_3$**

CD_3CN (400 MHz)

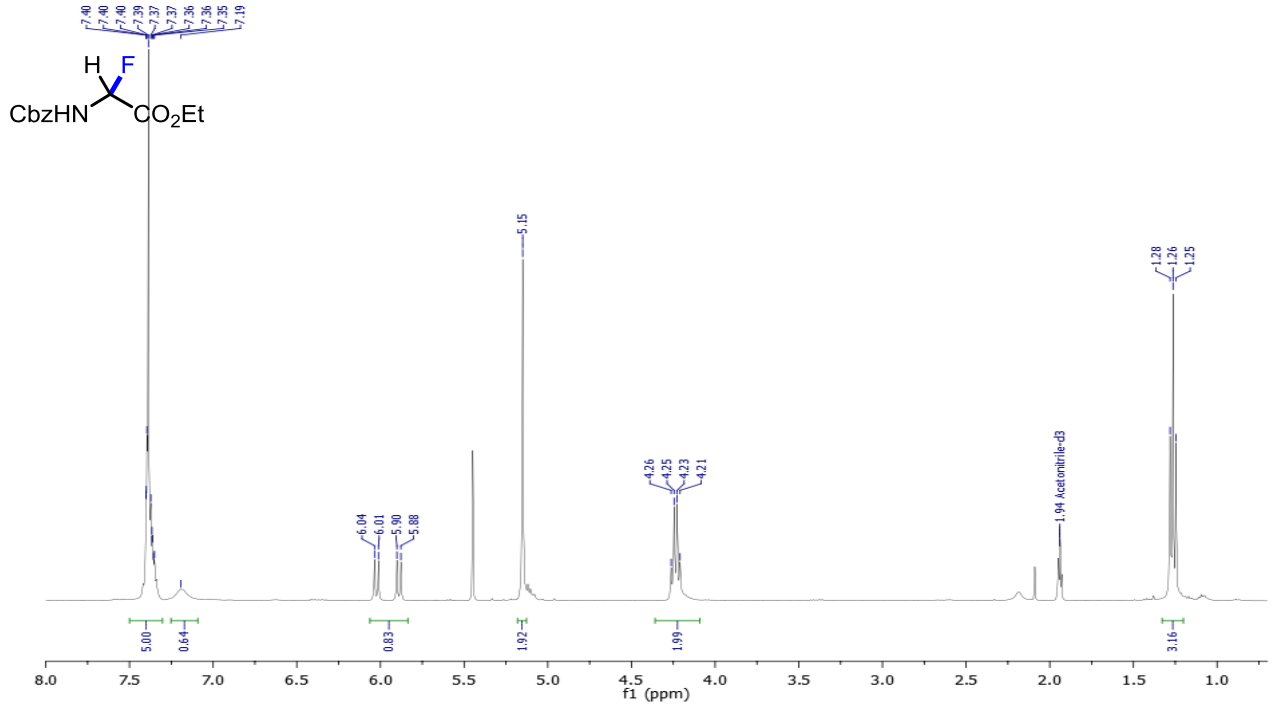

CD_3CN (100 MHz)

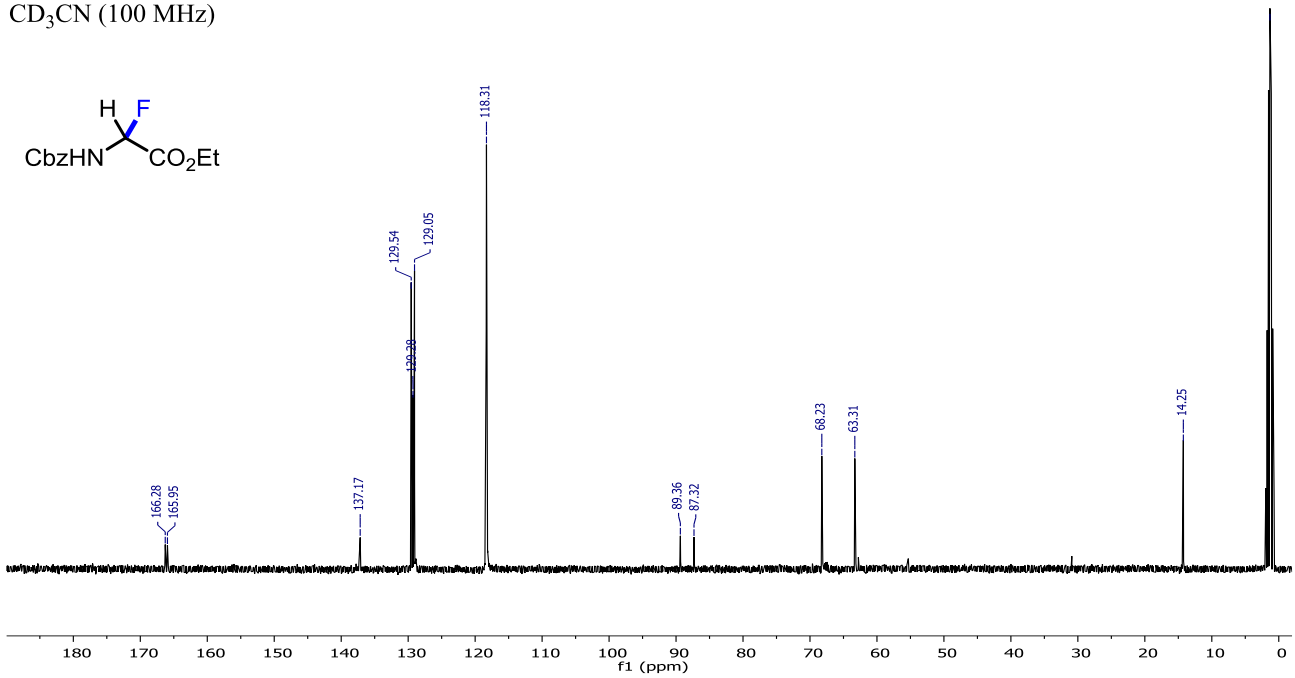

^{19}F NMR, $CDCl_3$ (377 MHz)

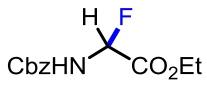

CD_3CN (400 MHz)

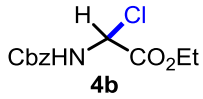

4b

$CDCl_3$ (100 MHz)

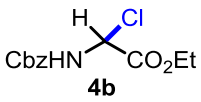

4b

CD_3CN (400 MHz)

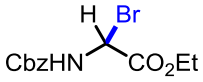

4c

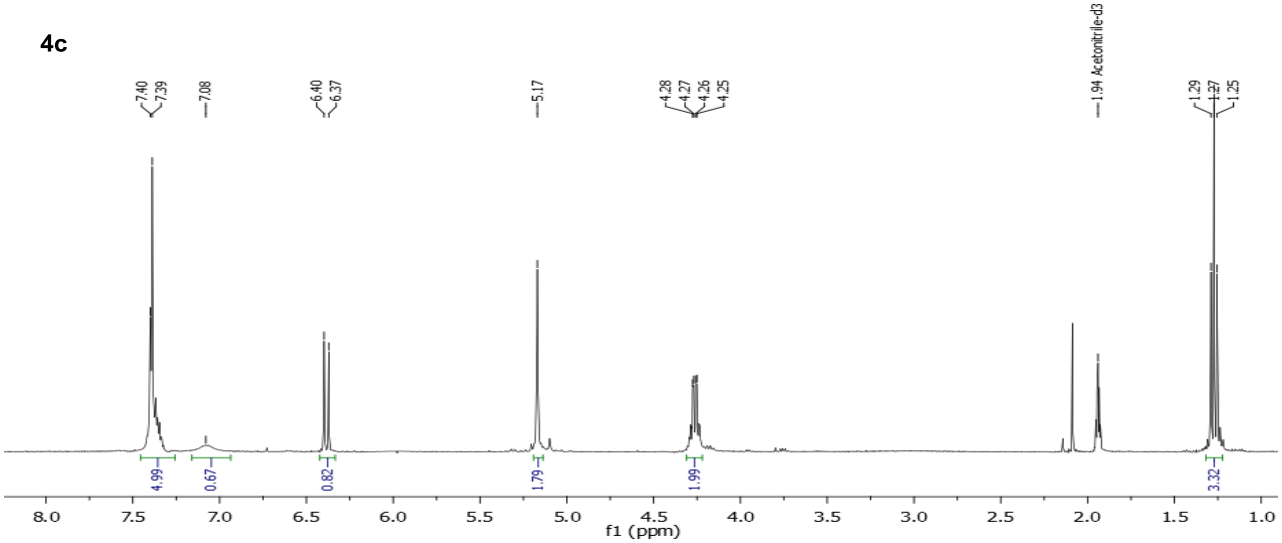

$CDCl_3$ (100 MHz)

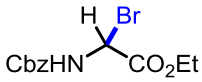

4c